DUPLICATE

Forecasting Research

Forecasting Research Division
Technical Report No. 91

Developments of the Mesoscale Model during 1993

by

P .A. Clark, S.D. Jackson, B. Macpherson, A. Maycock,
R.W. Robinson, R.N.B. Smith, S.A. Woltering, and B.J. Wright

April 1994

Meteorological Office
London Road
Bracknell
Berkshire
RG12 2SZ
United Kingdom

ORGS UKMO F
National Meteorological Library
FitzRoy Road, Exeter, Devon. EX1 3PB

Developments of the Mesoscale Model during 1993

FR Division Technical Report No. 91

April 1994

P.A. Clark, S.D. Jackson, B. Macpherson, A. Maycock, R.W. Robinson,
R.N.B. Smith, S.A. Woltering and B.J. Wright

Forecasting Research Division
Meteorological Office
London Road
Bracknell
Berkshire, RG12 2SZ
England

This is an unpublished document. Permission to quote from it must be obtained from an Assistant Director of the above Meteorological Office division.

Crown Copyright ©

Developments of the Mesoscale Model during 1993

FR Division Technical Report No. 91

April 1994

P.A. Clark, S.D. Jackson, B. Macpherson, A. Maycock, R.W. Robinson,
R.N.B. Smith, S.A. Woltering and B.J. Wright

Abstract

The mesoscale version of the Unified Model (UM), henceforth referred to as the MM, went operational in December 1992. Since that time work has continued to improve the model in a number of areas. This work has resulted in a number of changes to the operational model which were implemented at various stages in the autumn of 1993, together with a major change to the operational procedure (continuous assimilation) which will be implemented in spring 1994.

This Technical Report summarizes the development, testing and the expected impact of these changes. The motivation behind and the technical details of the changes are discussed followed by analysis of trial cases. The formulation of new diagnostics which are now being used operationally is described. Finally, the performance of the operational model since the implementation of most of the changes is discussed

1. Introduction

The mesoscale version of the Unified Model (UM), henceforth referred to as the MM, went operational in December 1992. Since that time work has continued to improve the model in a number of areas. This work has resulted in a number of changes to the operational model which were implemented at various stages in the autumn of 1993, together with a major change to the operational procedure (continuous assimilation) which will be implemented in spring 1994.

The purpose of this Technical Report is to summarize the development, testing and the expected impact of these changes. Specifically, the motivation behind the changes is discussed in section 2 while section 3 discusses the specific changes that have been implemented. Section 4 describes the formulation of new diagnostics which are used in the analysis of some of the trial cases discussed in section 5. Finally, the performance of the operational model since the implementation of most of the changes is discussed in section 6, followed by an overall summary in section 7.

2. Why make changes?

The motivation behind changing the operational model is, of course, to improve its performance. However improvements may arise in various aspects of its operation which may be more or less visible to the end user, so it is worthwhile considering in a little more detail the motivation behind the changes.

Shortly after becoming operational a few instances occurred of numerical instability in the model. As might be expected these occurred in strong wind situations, with particularly strong upper level jets and surface gradients. An example is shown in Fig. 1. The instability is very obvious in the surface pressure pattern, although its impact on other aspects of the forecast is far less clear. The pragmatic approach to curing this problem is to increase the damping introduced by artificial diffusion in the model. However, if this is achieved simply by increasing the artificial diffusion coefficient mesoscale detail will be lost unnecessarily. Increasing the order of diffusion is analogous to increasing the order of filtering, so that the high frequency cutoff is sharper. The high spatial frequencies, where instability first shows itself, can be smoothed without loss of intermediate frequencies, and so without the unnecessary loss of detail. With these considerations in mind, trials were performed increasing the order of artificial diffusion from ∇^2 to ∇^4.

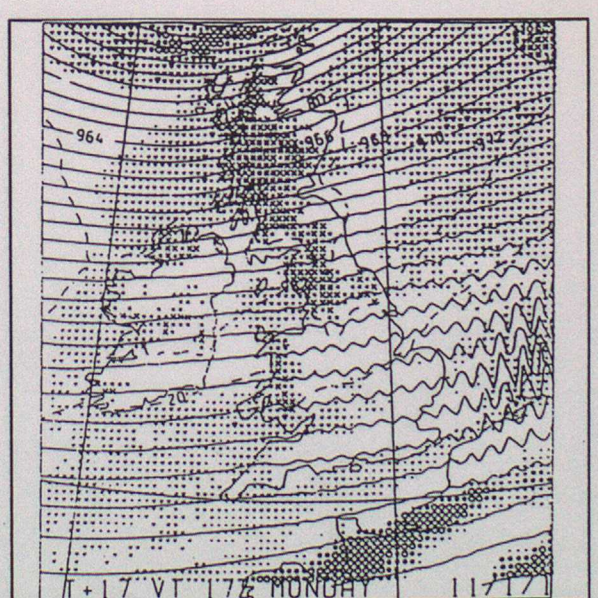

Figure 1 Example of instability in the operational run on 11/1/93.

In keeping with the unified approach to modelling, modifications arise from work on other model scales which may have benefit in the mesoscale. This was the primary motivation behind trials, and eventual implementation, of the 'frozen physics' configuration of the model (with some modifications). The unified approach, however, does not imply that all configurations of the model should be identical; indeed, it is expected that the scale dependent nature of some parametrisations should manifest itself as configuration dependent parameter values. The original operational MM used different values of convection parameters from the standard. However, after the implementation of changes to the convection scheme, experience suggested that the model had a tendency to overdo shower activity. A return to the standard convection parameters was therefore tested along with ∇^4 diffusion.

The MM went operational in December 1992 after having met specified user requirements for precipitation, 10 m wind and screen temperature. However, no requirements were specified for its performance with respect to visibility, fog and low cloud. Visibility and fog were handled quite well by the old Mesoscale Model (OMM) which had superior vertical resolution in the boundary layer and explicit treatment of aerosol analysis and transport. Not surprisingly, therefore, the performance of the MM was inferior to the OMM. On occasion the model failed to indicate any fog formation when widespread fog was present over much of the country. This had inevitable consequences on confidence in the model. A significant fraction of the work on the model has therefore been directed towards improving the fog and low cloud performance, in particular changes to vertical resolution and assimilation procedures. A User Requirement (UR) was formulated and agreed by the relevant parties and some of the discussion below will concern the degree of success in meeting this requirement.

The final motivation behind operational changes is to reduce the usage of resources. Following on from experience with the LAM, tests were performed using configurations of the MM which only call the convection scheme after multiple timesteps. The aim is to achieve a CPU saving without changing the forecast product (and thus perhaps free resources for other enhancements). Finally, the autumn saw the implementation of AutoMOPS, the automated form of the mesoscale cloud analysis scheme. This is intended to free forecaster effort without, again, having a detrimental impact on the forecast.

3. What has changed?

The operational changes were split into two main phases, partly to reduce the number of changes implemented at any one time and partly to aid the approval procedure.

Phase 1 : Operational 14th September 1993

- ∇^4 diffusion for u, v, θ and humidity, all with a coefficient of 3×10^6.
- Standard convective closure parameters.
- "Frozen Physics". Comprising

1) Removal of the assumption of random overlap of cloud in long wave radiation scheme (i.e. adoption of the maximum/random overlap assumption).
2) An improved numerical treatment of the non-local turbulent mixing scheme in the boundary layer, Geleyn surface layer interpolation and internally consistent surface layer treatment.
3) A fully divergent parametrization for ice in the precipitation scheme and different threshold liquid water contents for precipitation formation over the land and sea (8×10^{-4} and 2×10^{-4} kg m^{-3} respectively).

- Convection every alternate timestep.
- New fog and cloud diagnostics.
- Screen level RH assimilation.
- Revised assimilation parameters for temperature and RH data.

Phase 2 : Operational 2nd November 1993

- Automatic MOPS. (5th October 1993).
- Increased vertical resolution. Extra bottom level.
- Revised critical RH profile.

Minor Changes : Operational 8th December 1993

- Precipitation evaporation correction.
- Correction to remove spurious snow showers.

Proposed Future Changes

- Continuous Assimilation.
- Four runs a day.

4. Visibility, Fog and Cloud Diagnostics and Verification.

4.1 Visibility and Fog

Visibility was implemented as a diagnostic in a similar fashion to the OMM (Ballard, Wright and Golding, 1992). It is diagnosed using a semi-empirical relationship between relative humidity (RH) and visibility. This relationship also involves the number density of cloud condensation nuclei.

$$Visibility = \mathrm{vis}(RH, CCN)$$

The detailed relationship will not be discussed further here - the reader is referred to Ballard et al for details. The important point is that RH is effectively a model prognostic variable with a large dynamic range (diurnal, airmass etc.). The CCN concentration is, hopefully, much more conservative than RH. The OMM advected a single level boundary layer field from an initial analysis derived from the inverse of the above, so that many of the errors in this relationship were compensated for in the analysis. For example, if the relationship assumed an effective size which was too large, this would be compensated for by an erroneously large CCN concentration in the analysis. The MM, at present, fixes CCN as a parameter (200 cm^{-3}). Apart from not showing any airmass dependence, this implies that any errors in the relationship are not compensated for.

Fig. 2 shows the relationship between relative humidity and visibility currently used in the MM[1]. This shows that a visibility less than 1 km (defined as 'fog') is diagnosed at RH greater than 96.8 %. The threshold for 'mist', 5 km, is diagnosed at RH greater than 92.5 %. The relationship between visibility and RH is a fairly steep one, especially near (RH just below) the 1 km threshold. The diagnosis of visibility is thus very sensitive to model errors. The same is true of reality, in that near the 100% RH level, small RH fluctuations may lead to large fluctuations in visibility from place to place. In addition, observations are not as accurate as those of, say, temperature. As a result of all these sources of noise, objective verification of visibility tends to give a very pessimistic indication of the ability of the model to forecast fog.

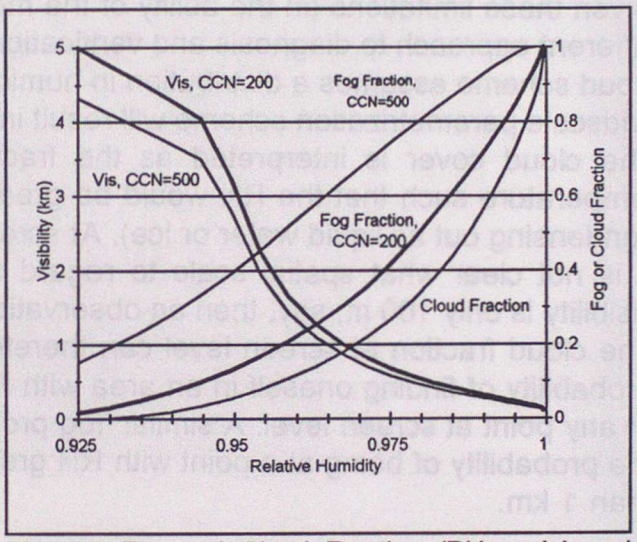

Figure 2 Fog and Cloud Fraction (RH scale) and Visibility (LH scale) in the MM for critical RH of 92.5% and CCN=200 and 500 cm^{-3}.

In addition to the obvious inadequacy of the simple relationship above, the scheme incorrectly assumes uniform relative humidity and hence visibility in a grid box. In practice the boundary layer scheme is used to derive a screen level RH so that the mean vertical profile is taken into account, but horizontal homogeneity is still assumed. Clearly, this is inconsistent with the present cloud scheme. In practice horizontal inhomogeneity is always present because of turbulent fluctuations together with variations in surface characteristics and orography which are not resolved by the model grid. Ignoring the latter terms, it should be noted that the model physics which lead to the RH prognosis in the first place assumes a distribution of humidity, such that at any RH greater than the critical RH, currently 92.5 % in the lower boundary

[1]This figure is calculated for a temperature of 5 C and pressure of 1013.25 hPa, but it is not very sensitive to these conditions.

layer, some liquid water is present in patches (Fig. 2). Irrespective of the accuracy of the model, for consistency with the model physics RH greater that 92.5 %, which would currently be diagnosed as mist, should be interpreted as patchy fog, with sub-gridscale patches. This, to some extent, explains the model's poor performance in some trials, as in situations in which only relatively small patches of fog were observed (so that not all stations showed fog in an area) the model was interpreted as showing no fog.

Verification of patchy fog on a scale larger than the grid size is also difficult. As the model orography is not the same as real orography, large (e.g. 30-40 km) patches may not coincide with actuality, even though the forecast gives very good guidance. Indeed, given the resolution of model orography, and the important role of orography in fog formation, it is unreasonable to expect the location or extent of fog to be forecast to better than a scale of 50 or so km.

Given these limitations on the ability of the model to forecast fog on a small scale, a different approach to diagnosis and verification of fog has been adopted. The current cloud scheme assumes a distribution in humidity within a grid box. (Indeed, any sub-gridscale parametrization scheme will result in some kind of distribution within a box.) The cloud cover is interpreted as the fraction of the box with total water and temperature such that the RH would be greater than 100% (the excess, of course, condensing out as liquid water or ice). At screen level, a cloud cover is meaningless. It is not clear what spatial scale to regard as relevant at screen level; when the visibility is only 100 m, say, then an observation is clearly only relevant on that scale. The cloud fraction at screen level can therefore be interpreted quite literally as the probability of finding oneself in an area with RH=100% and hence condensed water at any point at screen level. A similar 'fog probability' may be defined by considering the probability of being at a point with RH greater than that required for visibility less than 1 km.

Fig. 2 shows the MM relationship between fog probability and RH as well as the underlying cloud probability to show the influence of aerosol. It is evident that a visibility of 1 km based on the mean RH corresponds to a fog probability rather greater than 30 %. For this reason, as a working rule, a diagnosed fog probability of 30 % has been taken as indicating that a grid square is 'foggy', though this may be refined and is discussed further below in the light of trial and operation experience. The fig. also shows the visibility and fog probability for a value of CCN=500 cm^{-3}, which is not unreasonable for polluted air. This shows that the fog probability is much more sensitive to CCN than the currently diagnosed visibility.

It is important to emphasize that the concept of presenting a 'fog probability' and the method used to derive it are intended to be two entirely separate concepts. A direct relationship between the local RH distribution and the fog diagnostic has been used as a first step. However, this has its limitations. For example, it fails to distinguish between occasions when radiation fog is forming in a genuinely local and patchy fashion, (in which case a sharp surface inversion is likely to exist) and visibility is reduced over a wide area in a moist, probably particulate laden and fairly well mixed airmass. It may well be worthwhile, in future, refining the fog probability diagnostic by considering the vertical structure in the model near the surface. In addition, or

alternatively, it may be valid to tune the diagnostic in the light of operational performance. As will emerge below, it already appears to be the case that different fog conditions may be discerned from the diagnostic.

4.2 Stratus

Although, on occasion, more mobile in nature, stratus has many of the same properties as fog when it comes to diagnosis and verification. The presence of cloud below 1000 ft asl is of particular interest to aviation and may have many of the patchy qualities of fog, especially, of course, when it has arisen in the first place from lifting fog. A similar diagnostic product and verification scheme has therefore been defined. The diagnostic variable is simply the total fraction of the air between the surface and 1000 ft asl (pressure weighted) occupied by cloud. This may formally be defined as:

$$Stratus\ Probability = \int_{p_{1000}}^{p_*} C(p)\, dp$$

where p_{1000} is the pressure at 1000 ft asl , p_* is the pressure at the surface and C(p) is the cloud fraction at pressure p.

The bottom level of the model was included in this analysis as fog present at an observing site might well have lifted into stratus at an adjacent point, while stratus at one point may well be fog at a nearby (perhaps elevated) point. However, it should be noted that the fog probability is derived at screen level, while the stratus diagnostic only uses cloud amounts on model levels, so that it is possible to have a positive fog probability with no stratus, if the fog lies entirely under level 1. This should be born in mind when interpreting the charts, as the stratus probability, when significant fog is likely to be present, gives an indication of the vertical extent of the fog (i.e. the fraction of the distance from the surface to 1000 ft asl).

5. Trial Results

5.1 ∇^4 diffusion and Standard Convective Closure Parameters

A number of trials were performed on several cases using various versions of the model. These all gave very much the same impression of the impact of the modifications, but the conclusions here will draw upon the 'clean' tests at version 3.1 of the MM.

In general, neither ∇^4 diffusion or standard convection parameters have a dramatic impact on forecasts, although for the most part the impact is beneficial. ∇^4 diffusion has the expected effect of sharpening features such as troughs and convergence zones a little. This has a very minor impact on winds (as gradients tend to be increased) but the primary effect is on organized precipitation areas, which tend to be more active features. Small amounts of additional cloud are also produced, especially at medium level.

The use of standard convection parameters has little impact on precipitation from layer cloud but does tend to produce more low cloud. Not surprisingly, the most important impact is on shower activity, which is often reduced and generally is represented more realistically.

The combination of ∇^4 diffusion and standard convection parameters has quite a marked impact on precipitation. For example, in the 23rd August 1991 case, used as part of the original MM trial, the rainbands associated with the depression moving up the Irish Sea (Fig. 3) are better resolved and generally handled in a more realistic fashion, particularly as the forecast develops. The low is also a little deeper, a common feature of ∇^4 diffusion cases. Shower activity tends to be (beneficially) reduced, and structure in the shower activity better resolved. For example (fig. 4), on the 12th April 1993, the LAM produced showers more or less uniformly over the whole UK around midday. The operational MM was criticized for not really adding much to this: it produced widespread showers over much of England and Wales, and failed to reproduce a gap in the shower activity over central eastern England and Wales. The change to ∇^4 diffusion and standard convection parameters improves the forecast considerably. At 12Z the shower distribution is much more realistic, with the correct location of showers over England.

On the whole, the impact on objective verification scores is marginal. Precipitation scores are sometimes better, sometimes worse, but the difference is probably of little significance. Cloud cover forecasts are generally improved, as both factors tend to increase cover in a model which tends to under-forecast cloud. However, the impact is small and likely to be of little subjective importance.

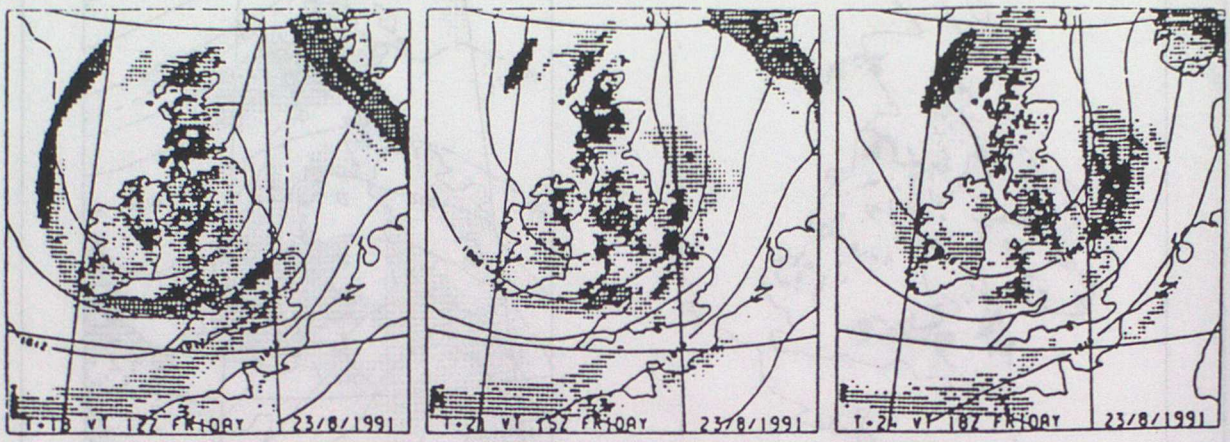

Operational Run

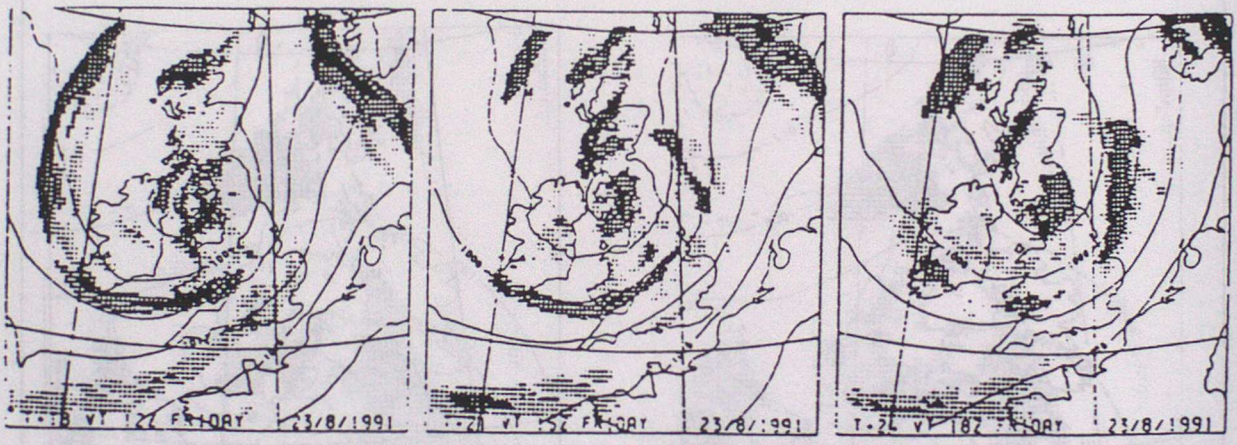

∇^4 and Standard Convection Parameters

12Z (T+12) 15Z (T+15) 18Z (T+18)

Figure 3 Comparison of operational configuration with ∇^4 +standard convection parameters for a forecast with DT 00Z 23/8/91

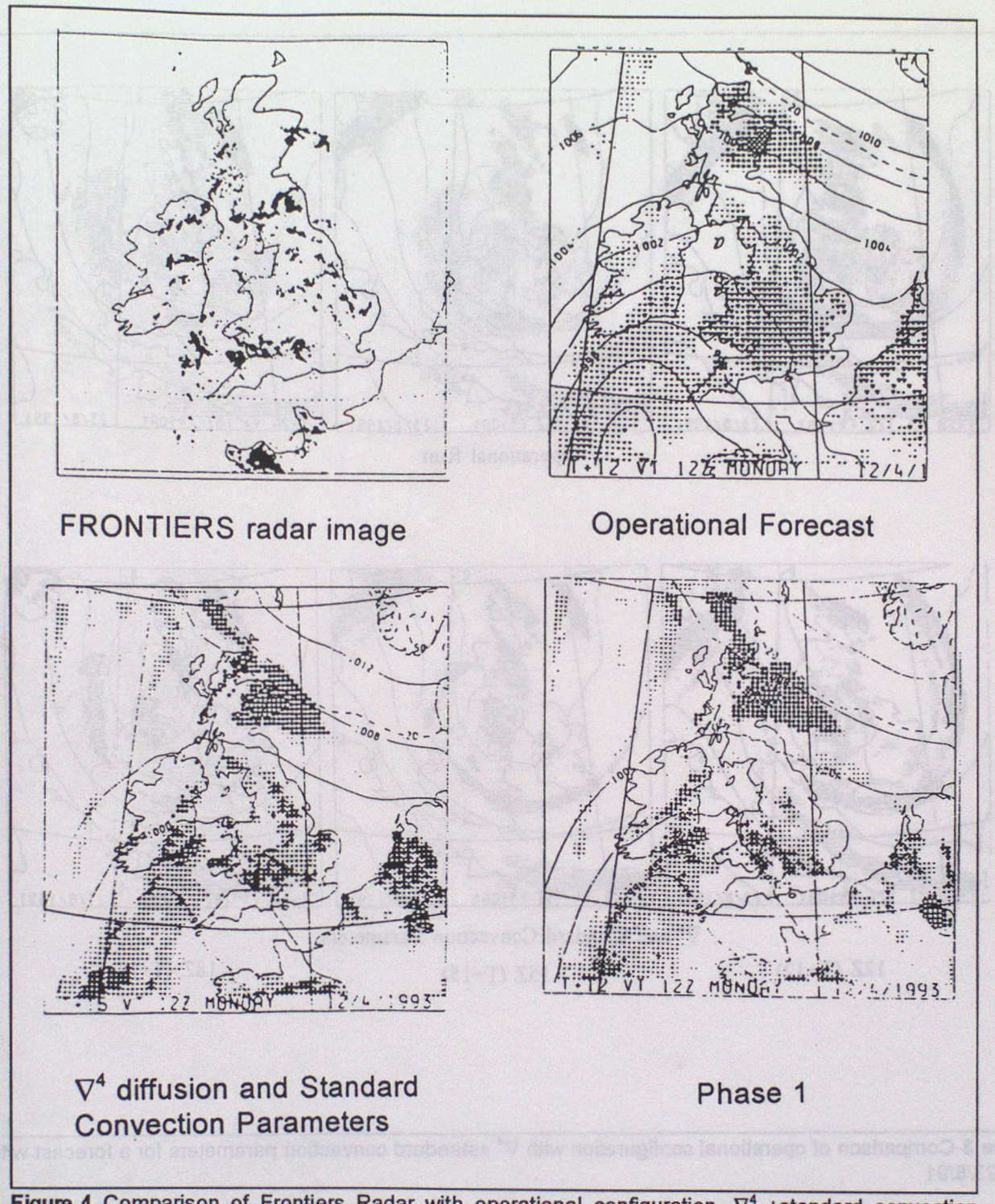

Figure 4 Comparison of Frontiers Radar with operational configuration, ∇^4 +standard convection parameters and "Phase 1" changes for a T+12 forecast with DT 00Z 12/4/93.

5.2 Convection called after multiple timesteps.

The convection scheme is a complex part of the model which is responsible for a substantial fraction of the CPU time in a typical model run. CPU time can therefore be saved by using the scheme more efficiently. It has been found with the LAM that it is feasible to avoid calling the convection scheme every timestep. Instead it is called every nth timestep and the same convective increments used for the subsequent n-1 timesteps. In order to work, this requires the changes in convective fluxes to be small over n timesteps.

Figure 5 Example of the impact of calling convection every 5 timesteps: Convective Cloud Top at T+30, from a forecast with DT 06Z on 8/11/91.

Five cases were studied involving convective activity. One case (8/11/91) was run calling convection every 10th step ("N=10"), but this failed so was not pursued. The same case was run at N=8. Although the same overall model evolution was followed, increasing noisiness was introduced as the forecast progressed. This was regarded as unacceptable. Similar noise and a tendency to break up convective structure were observed at N=5, which was run for three of the cases. Although the impact on the forecast in not very great, N=5 was not pursued further. All five cases were run with N=4 and N=2. In general, both gave acceptable results, although N=4 showed more tendency towards noisiness. Fig. 5 shows an example of the effect.

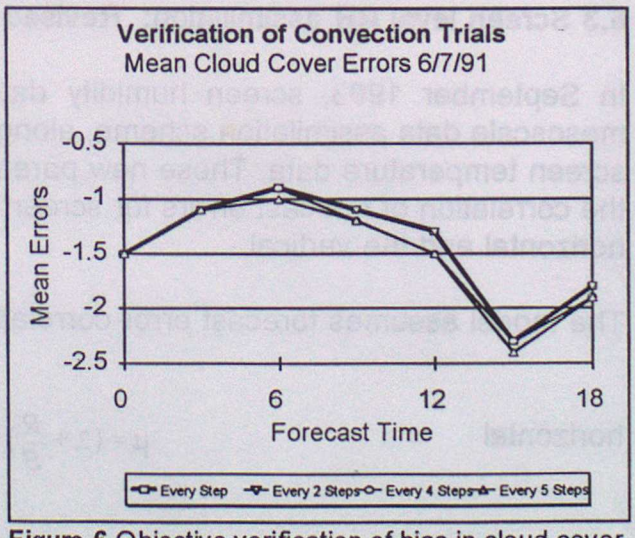

Figure 6 Objective verification of bias in cloud cover, 6/7/91, for runs calling convection every 1,2,4 and 5 timesteps.

A typical example of objective verification results is shown in Fig. 6 for the 6/7/91 case. The impact on verification is minimal. However, in general the difference between N=2 and N=1 is much smaller than the impact at N=4 and N=5. For the most part, it may be said that N=2 has negligible impact on the forecast while N=4 and above has a minor but more detectable impact. For this reason, N=2 has been adopted operationally. Should the need arise, N=4 could probably be adopted with reasonable confidence that the impact would be negligible. It would probably be wise, however, to consider other approaches to reducing the CPU time if the need should arise to go to N=4. For example, it has been suggested (Davies, personal communication) that running all the physics with a longer timestep, and just using a shorter timestep for dynamics (effectively the same as using a longer model timestep with split timestep dynamics) might reduce the noise problem by making all the physics mutually consistent. This is currently being investigated.

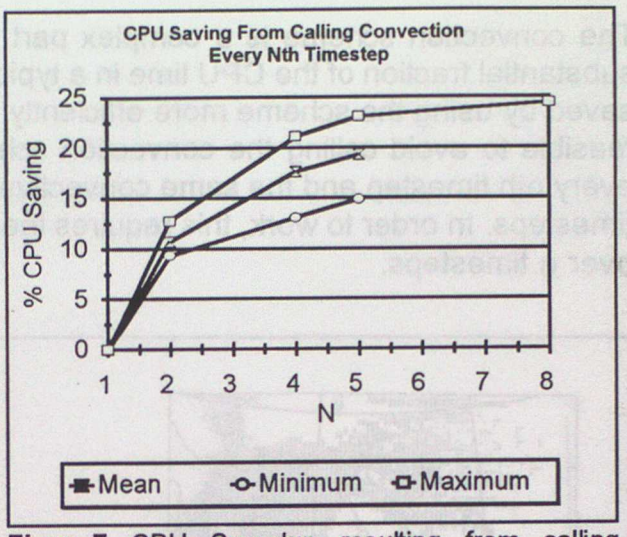

Figure 7 CPU Speedup resulting from calling convection every N steps. results from 5 cases.

The impact on CPU time clearly depends upon the amount of convection in a model run but is generally substantial (and, of course, is most when the model run is longest because of substantial impact of convection). Fig. 7 shows the CPU saving from the only run which included N=8, and the mean of all the runs (5 for N=2 and 4, 3 for N=5). Clearly the relative gain decreases as N increases as the absolute gain cannot be greater than the overall time spent in the convection routine. It appears that with N=2 a saving of about 10% can be expected in convective cases. A further 7% could be achieved by going to N=4.

5.3 Screen level RH assimilation: Revised Assimilation Parameters

In September 1993, screen humidity data were introduced into the operational mesoscale data assimilation scheme, along with revised assimilation parameters for screen temperature data. These new parameters were the result of work examining the correlation of forecast errors for screen temperatures and humidities, both in the horizontal and the vertical.

The model assumes forecast error correlations of the form:

horizontal $$\mu = (1+\frac{R}{S}) * e^{-\frac{R}{S}}$$

vertical $$\mu_I^m = e^{-b^2 \ln^2(\frac{P_I}{P_m})}$$

Here, μ represents a correlation, R is the station separation, S is the horizontal correlation scale, P_l and P_m are the pressures at model levels l and m, and b^2 determines the vertical correlation scale.

Using values of observation minus model background obtained from the OPD (Observation Processing Database), it is possible to produce distributions of error correlation as a function of station separation (or difference in levels in the case of the vertical correlation). Plots were produced for all main UK stations for four separate periods of time, 17th - 28th Feb., 1st - 31st Mar., 1st - 30th Apr., and 1st - 31st May 1993. Only SYNOP stations which had reported more than 80% of the time were used, and the study was confined to pairs of stations whose separations were within 400km. The result was the use of approximately 5000 station pairs. Correlation values were assigned to 'bins' of station separation for the horizontal study. Examples from the May results are presented in Fig. 8. For the vertical correlations, there were found to be 12 upper air stations in the mesoscale area which were considered to report frequently enough. Using the SYNOP reports collocated with these upper air stations, it was possible to obtain results for the correlation of (O-B) at screen level with (O-B) at higher model levels.

For both the horizontal and vertical correlations a curve was fitted to the data to obtain optimum values of the horizontal and vertical error correlation scales (S and b^2). By also obtaining the intercepts on the correlation axes, and using knowledge of the mean square (O-B) error averaged over all the stations, it is possible to calculate appropriate values for the observation and background errors. These errors are determined from the following formulae (Daley 1991):

$$E_b^2 + E_o^2 = \frac{1}{K} \sum_{k=1}^{k=K} \overline{(O-B)_k^2}$$

$$\mu_0 = \frac{E_b^2}{E_b^2 + E_o^2}$$

where μ_0 is the intercept at zero separation found by extrapolation of the curve best fitting the data for correlation as a function of separation, E_o and E_b are the observation and background errors, and the summation is simply the station averaged mean square (O-B) (for the set of k stations).

A summary of all the derived values can be found in the following tables.

MONTH	$\overline{(O-B)_k^2}$	μ_0	S (km.)	E_o (°C)	E_b (°C)	b
February	4.08	0.720	122.2	1.1	1.7	14.8
March	4.04	0.555	149.3	1.4	1.5	20.4
April	2.45	0.601	133.9	1.0	1.2	23.4
May	2.47	0.562	121.2	1.0	1.2	20.6

Summary of results for screen temperature correlation study.

MONTH	$\overline{(O-B)_k^2}$	μ_0	S (km.)	E_o (%)	E_b (%)	b
February	101.7	0.460	77.0	7.4	6.8	11.4
March	102.0	0.557	101.8	6.7	7.5	16.4
April	54.7	0.584	79.2	4.8	5.7	19.1
May	75.1	0.563	89.2	5.7	6.5	17.0

Summary of results for screen humidity correlation study.

Values currently used operationally are screen temperature observation and background errors of 1.1 and 1.4 degrees, screen humidity observation and background errors of 6.2 and 6.6%, a 'b' value of 18.0 for both temperature and humidity, and S values of 110km. and 75 km. for screen temperatures and humidities respectively. For both, data are analyzed on the bottom 6 model levels, experiment showed that by model level 6 the correlations had decreased to about 0.3.

Three mesoscale cases were run with and without the new assimilation parameters, and objective verification scores were obtained for screen temperatures and humidities (Fig. 9). They show a significant reduction in RMS screen humidity error at least out to T+6. Although there is an increase in the volume of data being used (i.e. the inclusion of screen humidity data), there is no overall increase in CPU time because of the reduction in the influence area of screen temperatures. The temperature verification at T+3 and T+6 shows one case with lower RMS error, one with higher error, and the third with negligible change.

5.3 Screen level RH assimilation: Trial Results

The primary aim of introducing the assimilation of screen RH is to improve the analysis and forecasting of low cloud and fog, although there may, of course, be

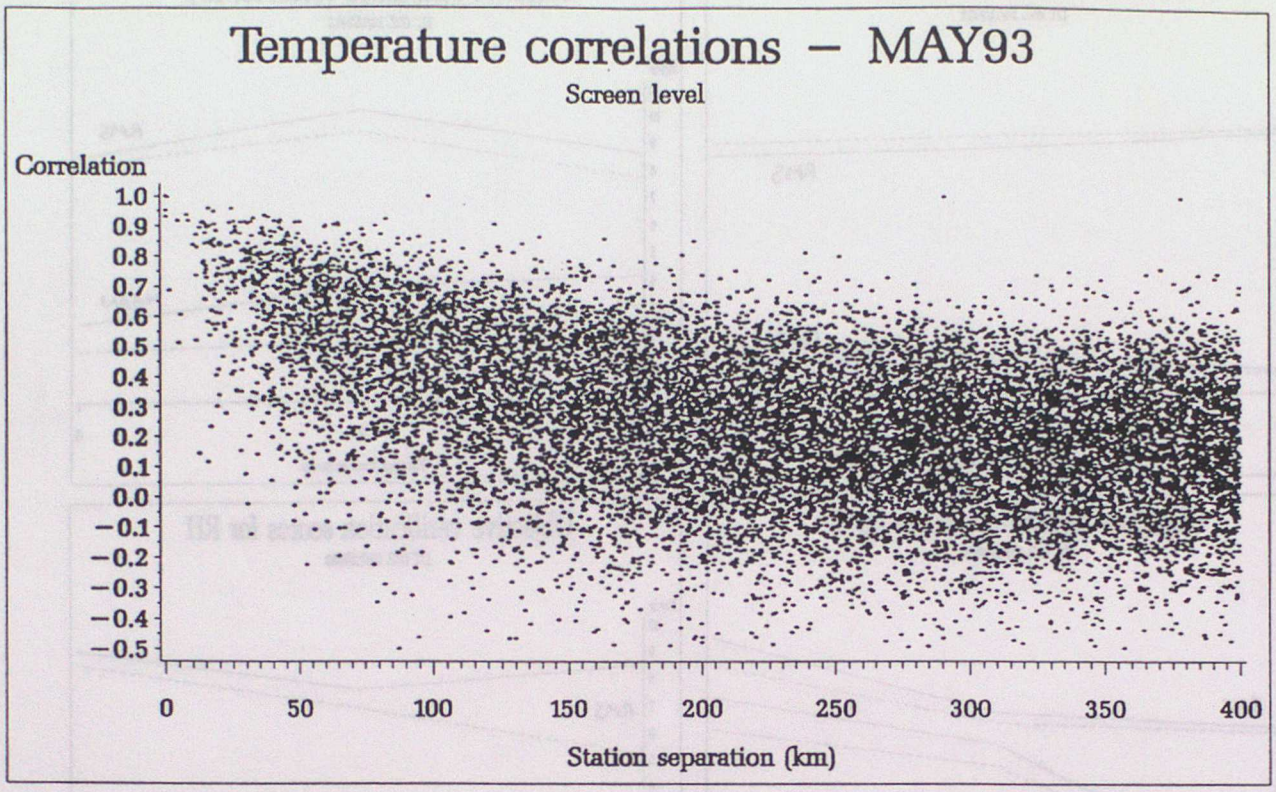

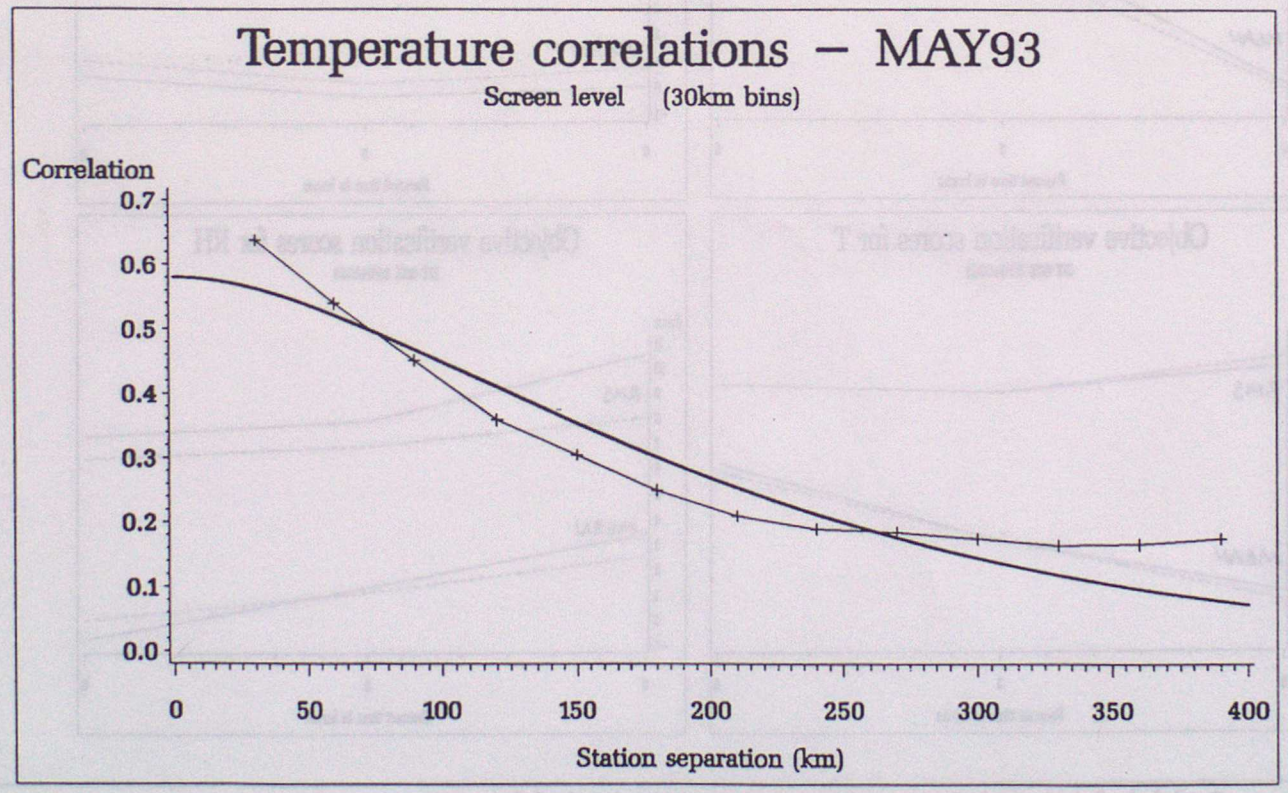

Fig. 8 Temperature correlations as a function of station separation: May 1993. In the lower plot, the curve indicated by crosses shows the data averaged into bins of 30 km station separation, the solid curve shows the best fit to these data.

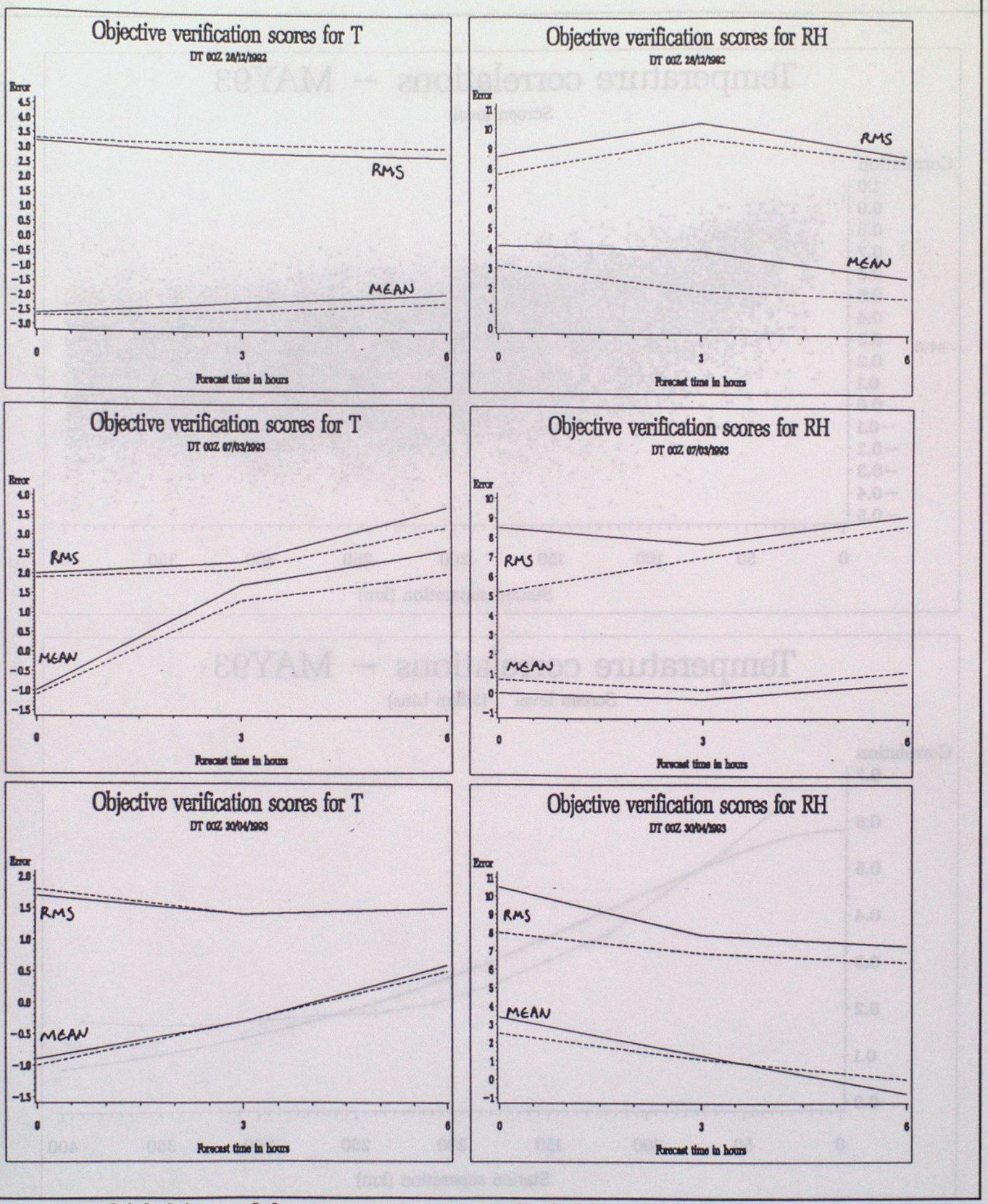

Solid line=Old parameters : Dashed line=New parameters

Fig. 9 Comparison of Objective Verification scores with and without new assimilation parameters.

06Z

07Z

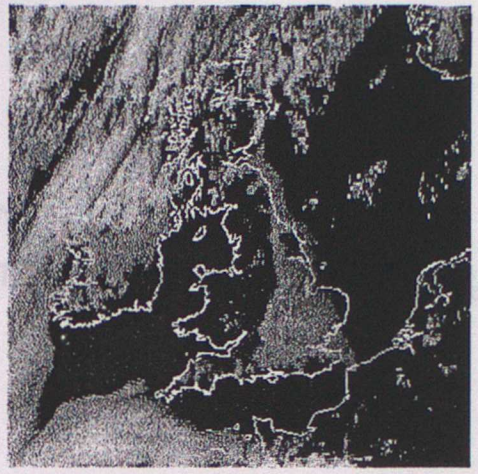

08Z

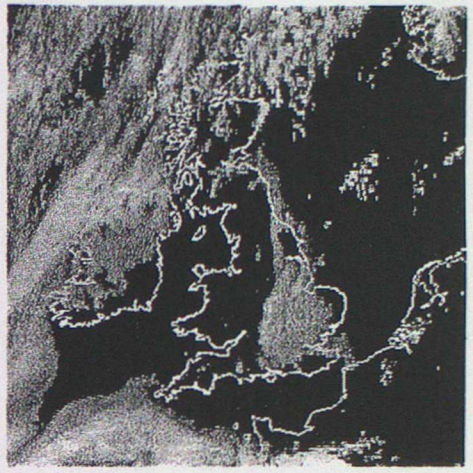

09Z

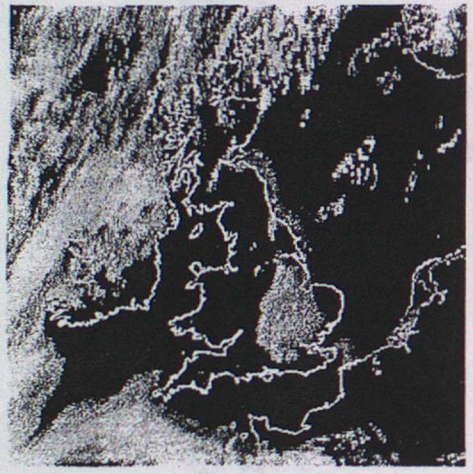

10Z

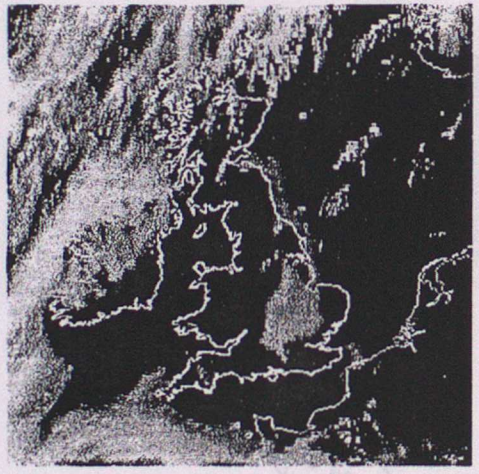

11Z

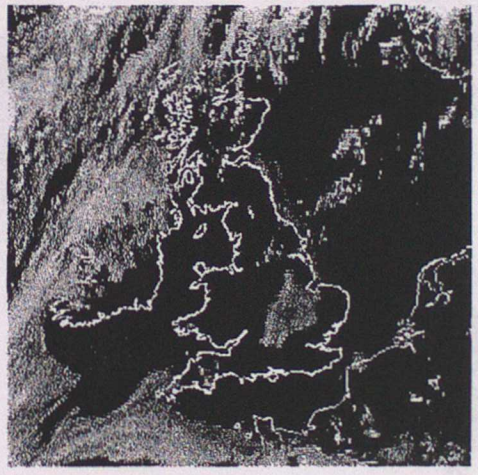

12Z

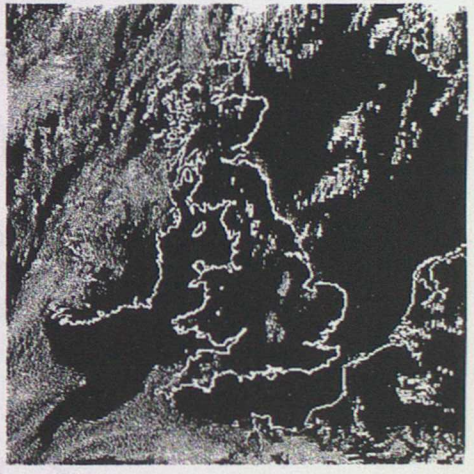

13Z

Fig. 10 Visible METEOSAT Imagery, 30/04/93

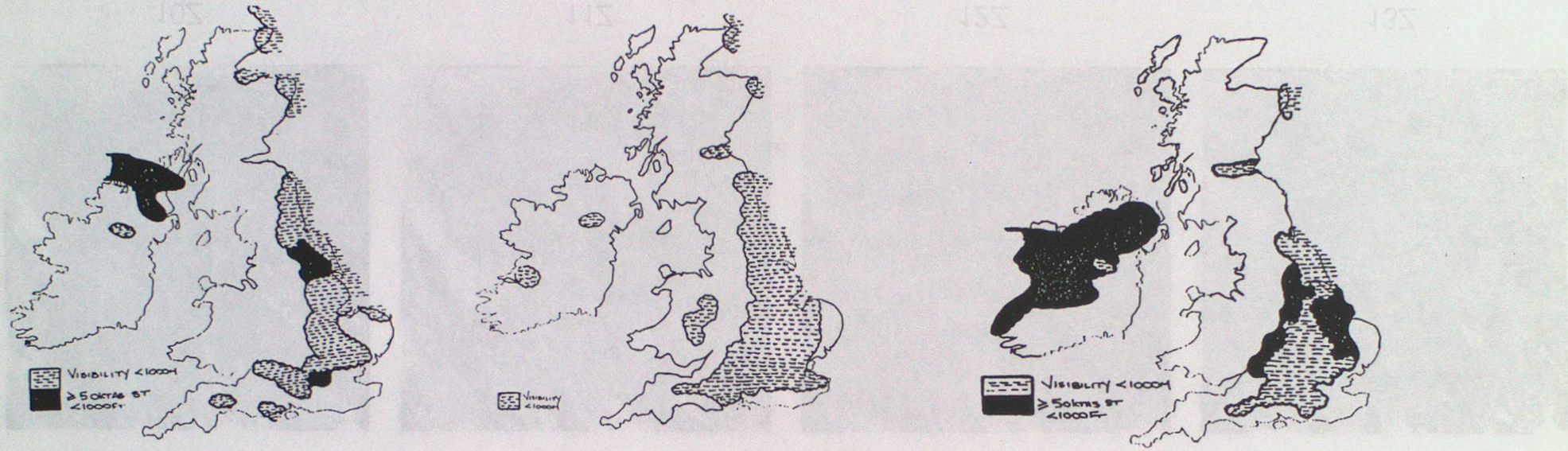

Fig. 11 Summary of 30/04/93 surface observations of fog and stratus.

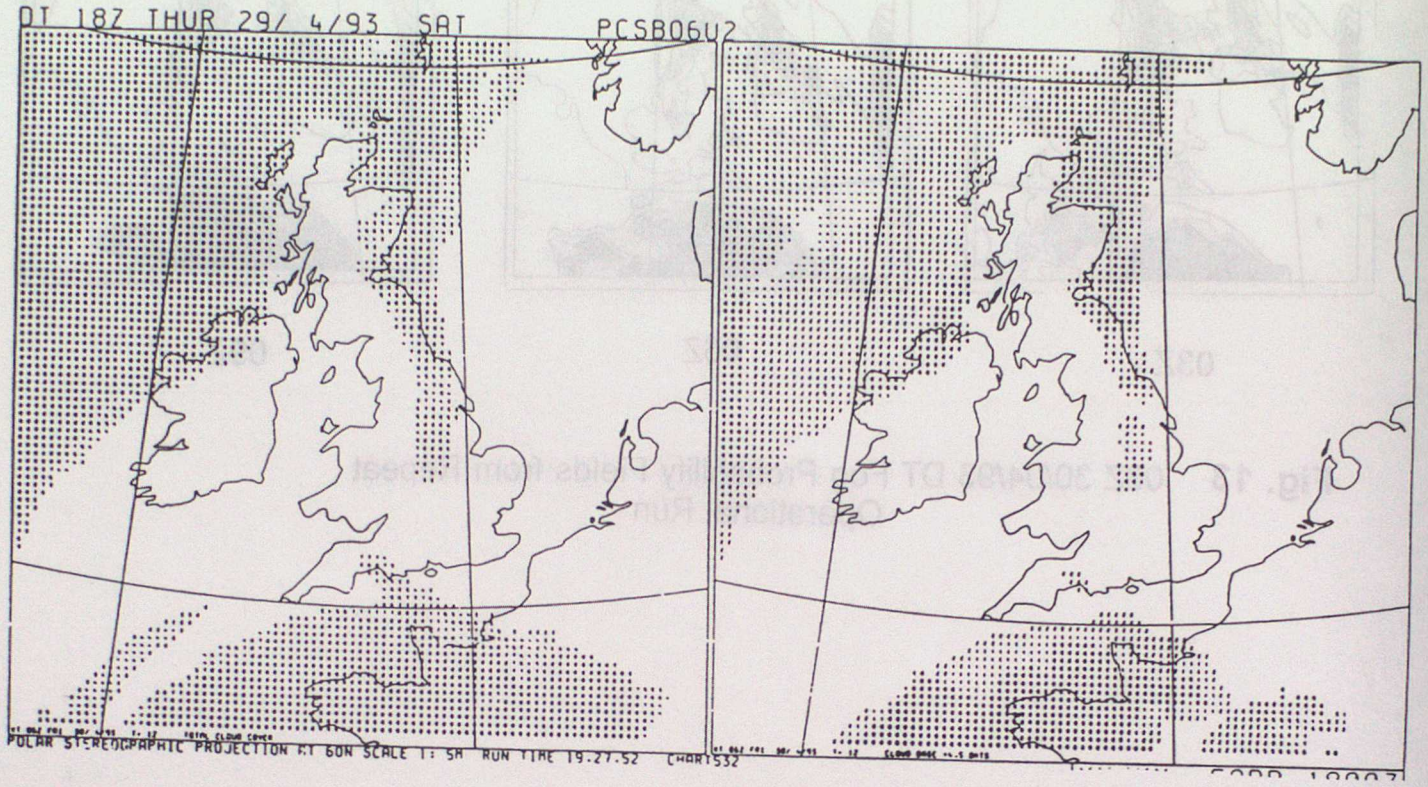

06Z Total Cloud

06Z Cloud Base > 4.5 OKTAS

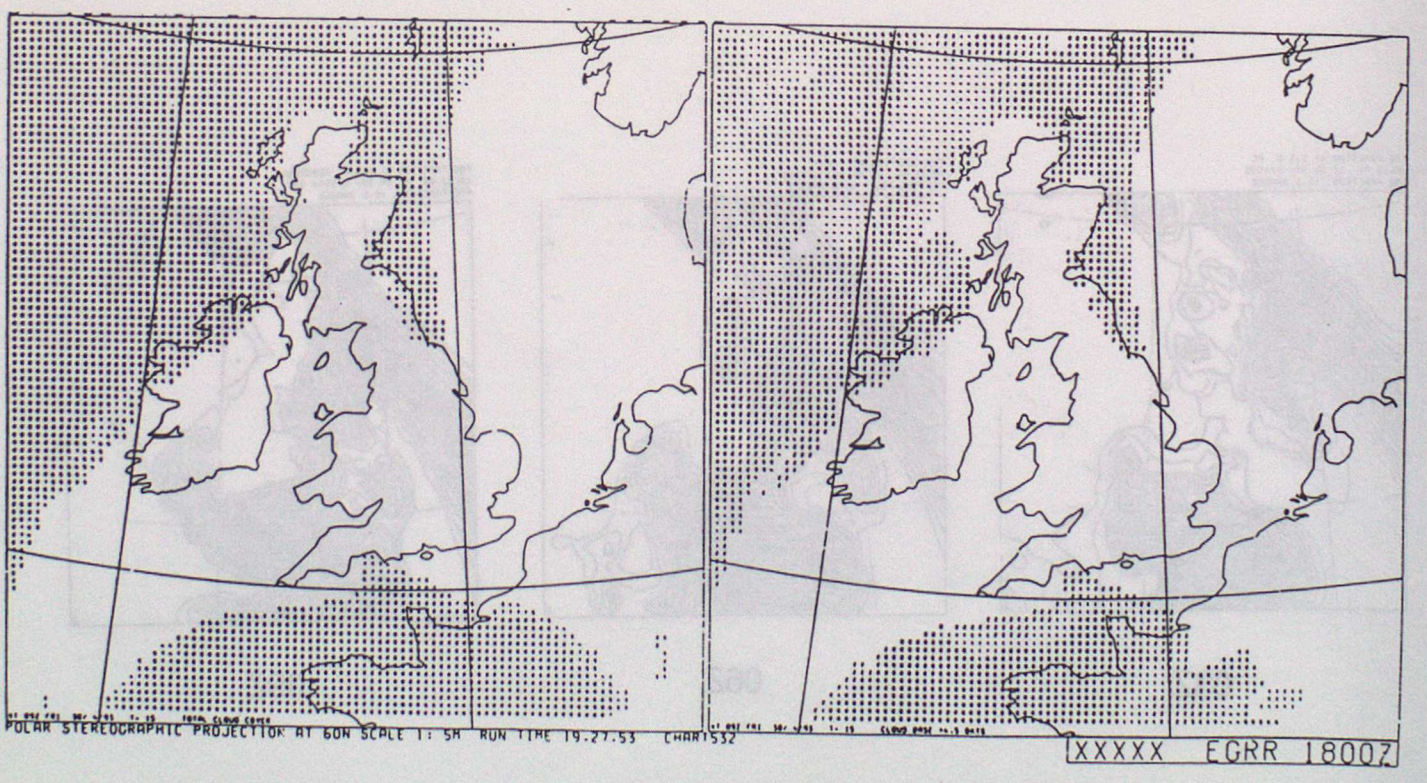

09Z Total Cloud

09Z Cloud Base > 4.5 OKTAS

Fig. 12 00Z 30/04/93 DT Operational Cloud Fields

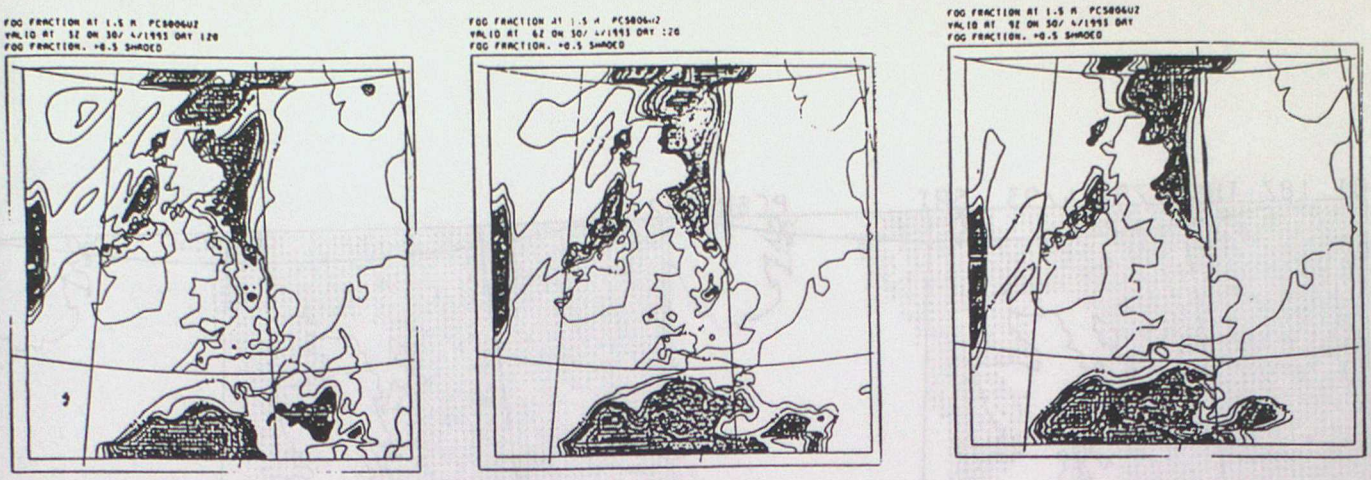

03Z 06Z 09Z

Fig. 13 00Z 30/04/93 DT Fog Probability Fields from Repeat Operational Run

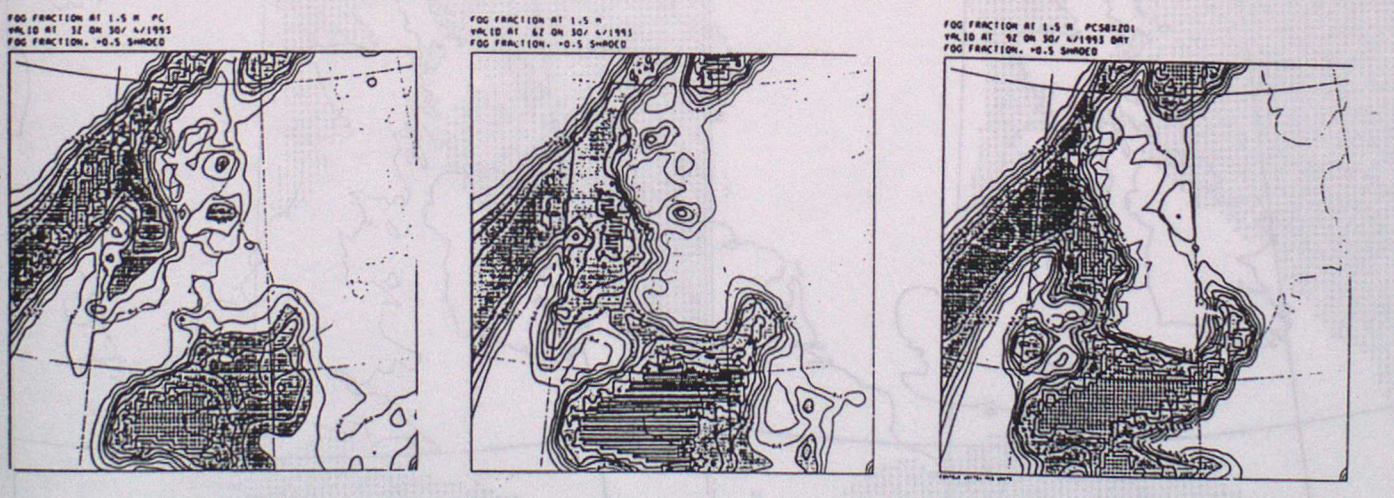

03Z 06Z 09Z

Fig. 14 00Z 30/04/93 DT Fog Probability Fields from Repeat LAM Run

additional benefits. With this in mind, the impact of screen RH assimilation has been assessed primarily in three cases, two characterized by fog and one by low cloud. One of these cases, 14/12/91, formed part of the original trial. The other two were chosen because they were good examples of the operational model performing particularly badly. The fog case, on 30th April 1993, will be considered in some detail as it contains many of the aspects of interest in fog forecasting, such as the formation of radiation fog, subsequent development into a thick layer over a wide area, followed by subsequent lifting into stratus and eventual dissipation.

The 30/04/93 Case

The area of fog formation on 30/04/93 is well illustrated by Fig. 10, which shows a sequence of visible METEOSAT images from 06Z to 13Z. The images have been enhanced to show the low cloud more clearly. These show an area of low cloud or fog covering much of eastern England gradually clearing (primarily after 09Z) until by 13Z only a couple of thin patches are visible. It is particularly interesting that to the north of England the fog is bounded by the Pennines and does not extend over the North Yorkshire Moors. A strip of thin fog extends up the east coast as far as the Firth of Forth, where, on the earlier frames, it extends inland. Although on the original imagery it is evident that this coastal fog is thinner than that over land, it was much more persistent, lasting through most of the day. The area of persistent fog or stratus over Ireland is also of note.

This imagery is valuable in showing the extent of the area, but, of course, cannot show any information before sunrise (indeed, the 06Z image has been heavily processed to extract the information), and cannot distinguish between fog and stratus. The surface observations of fog and stratus from 03Z, 06Z and 09Z are summarized in Fig. 11. This shows that the fog was still becoming established at 03Z (it had been absent at 00Z, the model analysis time), while by 09Z it was beginning to lift into stratus at the edges.

No fog or visibility charts were available in the operational MM run. However, the 06Z and 09Z cloud fields (Fig. 12) illustrate the problem. Some fog and stratus is present over Lincolnshire and Nottinghamshire, and extends over the north east up into the Firth of Forth. However, the southward extent is nowhere near enough, and by 09Z England is entirely clear. A rerun of the model in operational configuration (to ensure a clean comparison with subsequent tests and to extract a full set of diagnostics) produced fog probability charts shown in Fig. 13. The sea fog off the north east, and its encroachment into land, are quite well handled. The fog over Ireland gives a useful indication but is rather underdone. Over England, the fog probability gives a hint of fog in the right areas at 03Z, mainly in the 10-30 % range, and probably represents a useful if underdone forecast. It does illustrate that the fog charts would probably have been of value to forecasters. However, by 06Z the (low probability) fog area has shrunk considerably, and has gone by 09Z. Thus, although the model was trying to form fog in the right areas, by sunrise not enough had formed to prevent the sun burning it off very rapidly.

It is evident that, for whatever reason, the relative humidity was too low in the model as fog formed. Observations showed that the model temperature in the foggy area was

quite accurate at 06Z (roughly sunrise), even though it was too high later on (as a result of missing the fog). It is instructive to consider the behaviour of the LAM run over the same area. Fig. 14 shows the fog probability derived from the LAM run. While the fog over Ireland is handled quite well, that over England is treated very poorly. It appears that what fog there is (which is almost exactly in the wrong place) is largely an area of sea fog forming over the less well resolved LAM Channel. The temperatures over central England are about 2° too cold, so it is difficult to argue that the MM failed to form enough fog because the initial conditions were too warm. Indeed, it is evident that the initial conditions from the LAM were both too cold and too dry.

Without any assimilation (but including ∇^4 diffusion) the model retains many of the features of the LAM run during the night: at 3Z the temperatures are fairly similar, although the fog has cleared somewhat from the SW and is being controlled more by the MM orography and land-sea mask (Fig. 15). By 06Z, temperatures over central England have increased to agree fairly well with observations, indicating that the model response to sunrise was quite realistic. Since no data were being assimilated, this rise (compared with the LAM) must result from the increased resolution of the model. The surface characteristics are essentially the same as the LAM, so it is most likely that the much increased vertical resolution is responsible for the improvement. This is to be expected as the increased vertical resolution will allow the erosion of the nocturnal surface inversion after sunrise to be treated more accurately. Inclusion of assimilation of screen temperature improves the screen temperature at 06Z somewhat further. However, warming up to roughly the correct temperature, both from the model evolution and assimilation, prevents the formation of fog as the model relative humidity does not respond in parallel..

Assimilating screen RH in addition to screen temperature goes quite a long way towards rectifying the problem. Fig. 16 shows the fog probability charts corresponding to the operational run (Fig. 13). The 06Z chart shows much more developed fog in very much the right area. The spatial extent is still not enough: the 10% line encloses much, if not all, of the fog area but the model clearly should indicate greater probability. This is reflected in the 09Z chart, which shows much of the fog dissipated. It should be noted that the improvement in fog is not simply a result of assimilating fog over land at the outset. The 03Z chart is very similar to the operational run, if anything slightly less foggy. The screen temperatures (Fig. 17) at 06Z are also not very different between the two runs. However, by 09Z the impact of the fog in delaying surface warming is evident. A comparison of the analyses between the operational run and the run with ∇^4 diffusion and assimilation of surface RH shows that the RH distribution is markedly different (Fig. 18). Over much of the land area to the west of England the RH is actually reduced. Over land, it is only over the area of Lincolnshire and East Anglia that the relative humidity is markedly increased. However, the increase in RH extends upwind over the sea for a considerable distance. This served to increase fog over the sea and also to feed moist air inland as the forecast progressed through the first few hours. The spatial influence of the RH correction over the sea is probably mainly determined by the horizontal error correlation scale, since no surface RH measurements are assimilated over the sea.

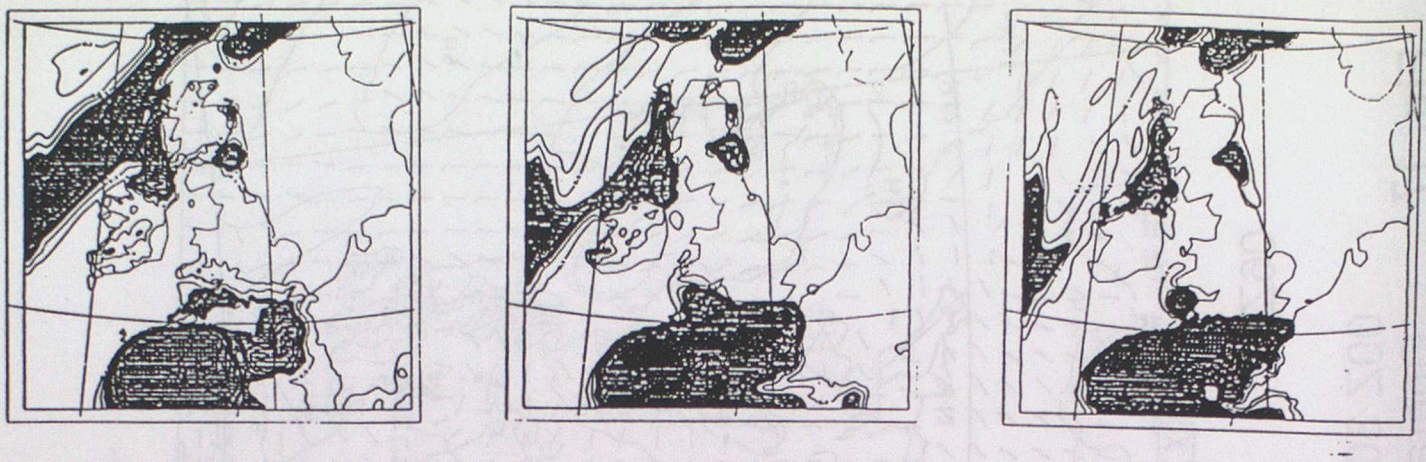

03Z 06Z 09Z

Fig. 15 00Z 30/04/93 DT Fog Probability Fields : Operational plus ∇^4 **without** assimilation.

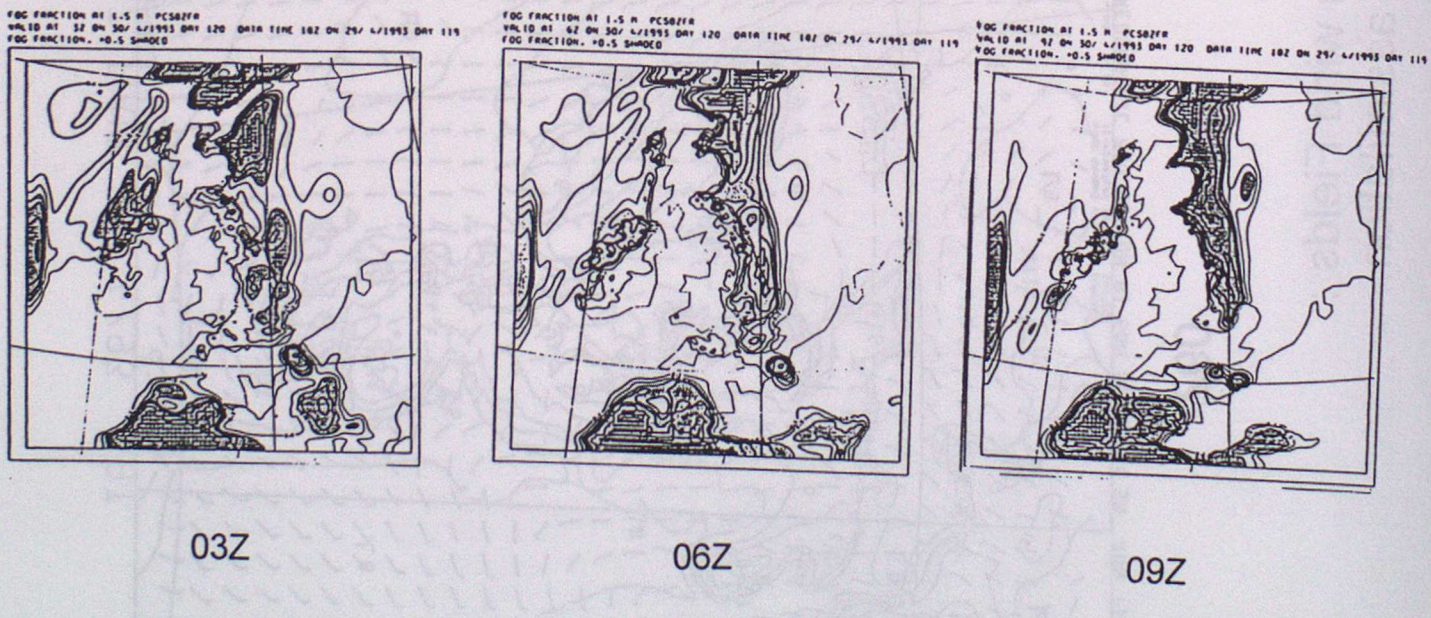

03Z 06Z 09Z

Fig. 16 00Z 30/04/93 DT Fog Probability Fields : Operational plus ∇^4 and screen RH assimilation.

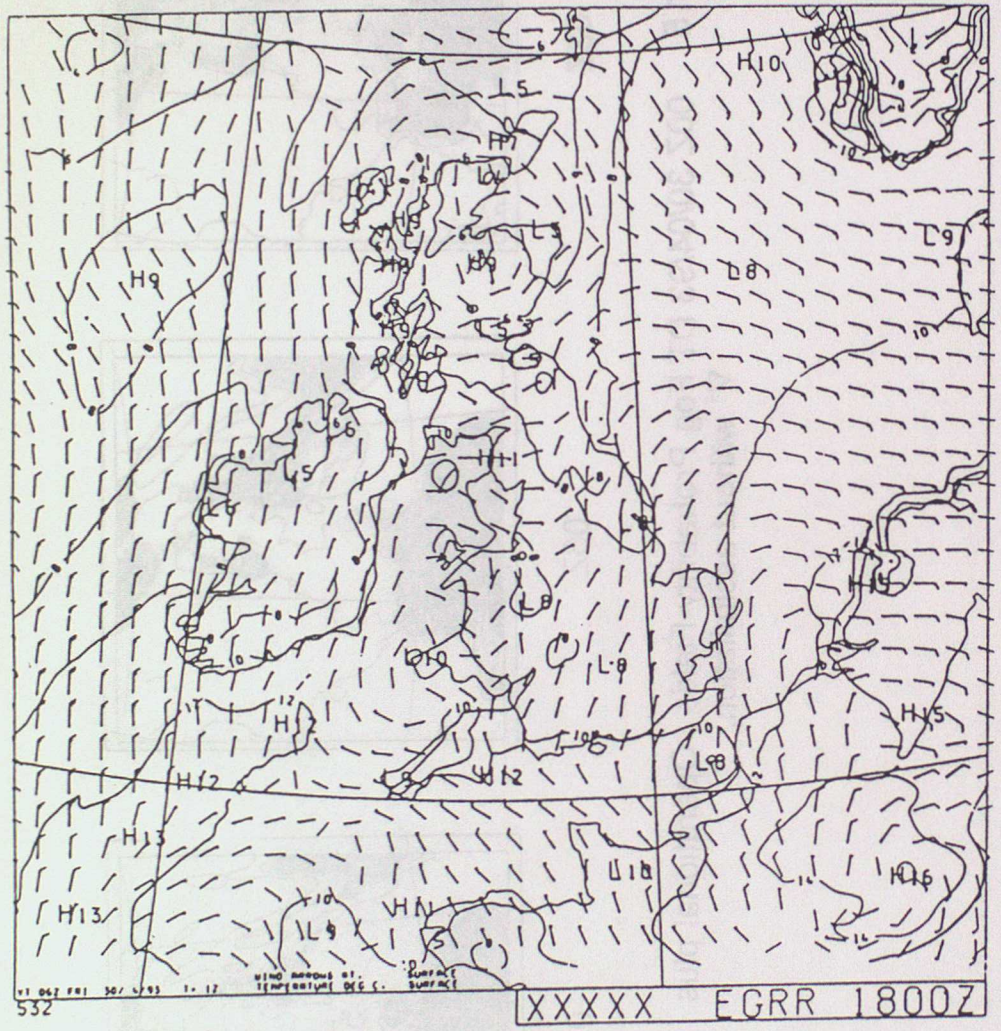

06Z

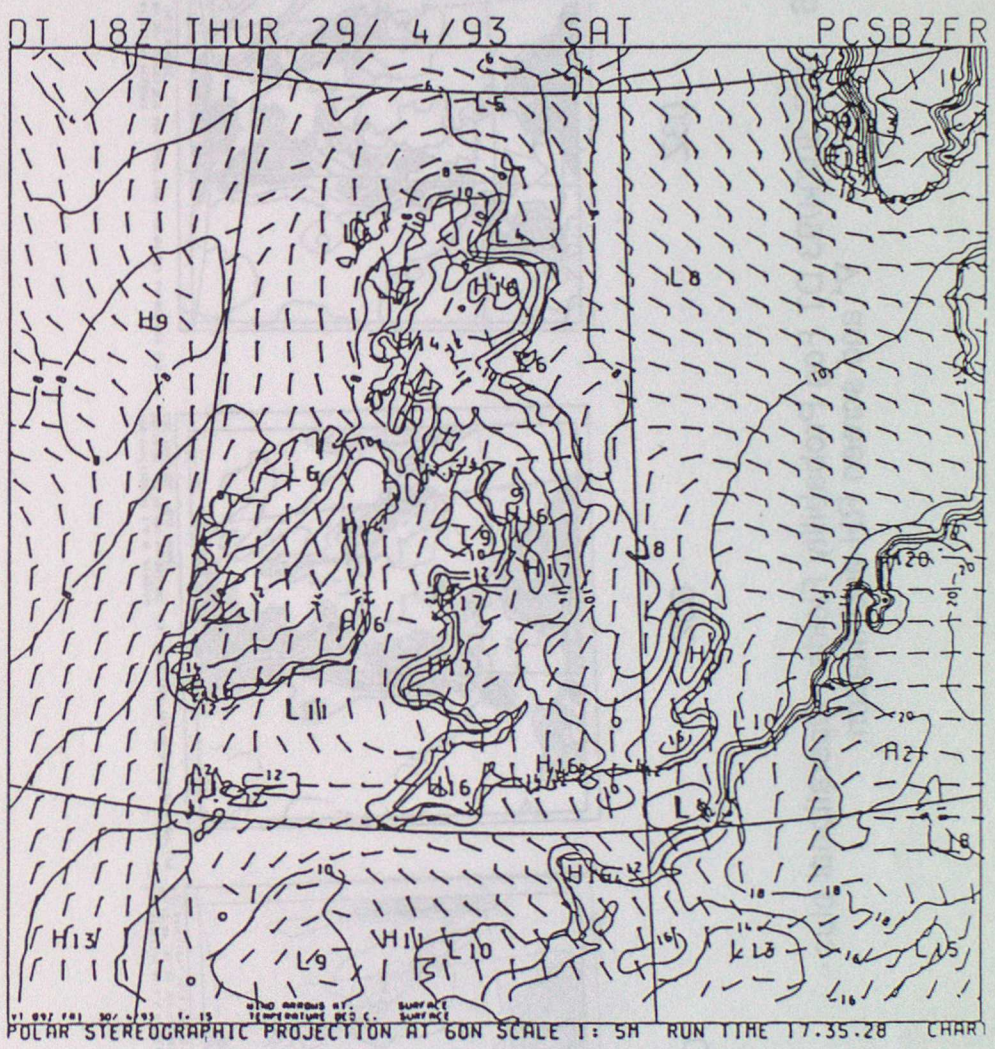

09Z

Fig. 17 00Z 30/04/93 DT screen T and 10m wind Fields : Operational plus ∇^4 and screen RH assimilation.

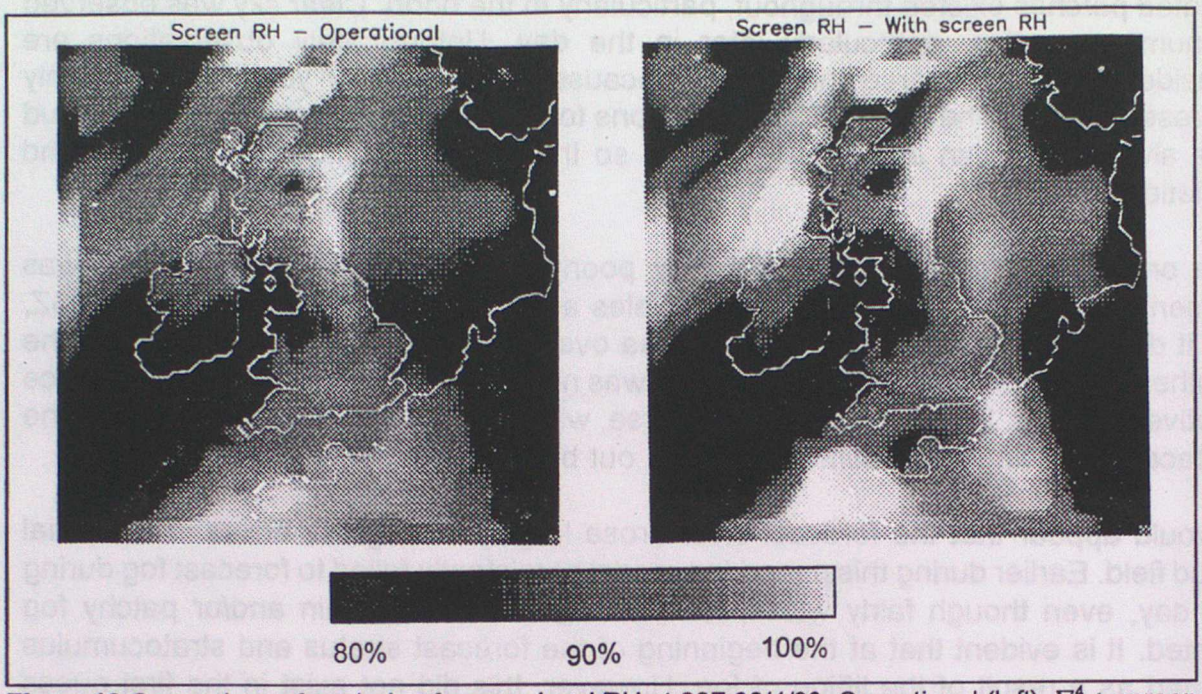

Figure 18 Comparison of analysis of screen level RH at 00Z 30/4/93. Operational (left), ∇^4 + screen RH assimilation (right).

14/12/91 Case

This was previously used in the mesoscale model proving trials. In this case, widespread (though later on patchy) frozen fog persisted throughout much of the day, finally dissipating around midnight (Fig. 19). The original model did not perform well in this case, as it loses fog during the afternoon. Assimilation of surface RH results in a noticeable improvement. The assimilation produces quite realistic fog cover. By T+3 this is similar to the operational run but includes an apparent gap around the Cambridgeshire/Northamptonshire area. In the operational run much of this fog had dissipated by 21Z, and all by 00Z on the 15th, even though fog was observed over much of eastern England at 21Z and over East Anglia at 00Z. The operational run produced spurious fog over western Scotland, Wales, the south west and Ireland. This remained in the rerun with RH assimilation, but the model succeeds in retaining an indication of fog over East Anglia and southern Lincolnshire throughout the day, keeping fog over East Anglia at 00Z. (Fig. 20). In other respects the runs are very similar, except in those variables directly affected by fog (such as screen temperature).

28/12/92 Case

This case was chosen as an example where the operational MM failed to forecast an area of widespread stratus. The impact of assimilation of surface RH was more disappointing. Fig. 21 shows the progress during the day. During the early hours of 28/12/93 stratus and stratocumulus was fairly widespread over a band running through

central England. This thinned out and became more patchy as the day progressed but isolated patches existed throughout, particularly in the north. Clear sky was observed at numerous sites, particularly later in the day. Unfortunately observations are considerably more sparse than usual because of the time of year. This probably represents one of the more difficult situations for the model to deal with, as the cloud was always of a thin and patchy nature, so that much depends on the cloud and radiation scheme.

The original operational model did very poorly. Some widespread low cloud was present over the west Midlands, north Wales and the southern Pennines up to 06Z, but it dissipated by 09Z except for an area over the North Yorkshire Moors and the southern Pennines (Fig. 22). The forecast was not improved by assimilation of surface relative humidity. In fact it was slightly worse, with low cloud being largely absent, the surface RH having been somewhat dried out by the assimilation.

It would appear that the forecast error arose largely from gross errors in the initial cloud field. Earlier during this period the model persistently failed to forecast fog during the day, even though fairly widespread, though sometimes thin and/or patchy fog existed. It is evident that at the beginning of the forecast stratus and stratocumulus existed as a result of the lifting of fog. However, this did not exist in the first guess field for MOPS. The impact on the cloud cover verification is shown in Fig. 23. As suggested, the forecast is slightly worse but the difference is small compared with the already very poor forecast (which. incidentally, improves with time).

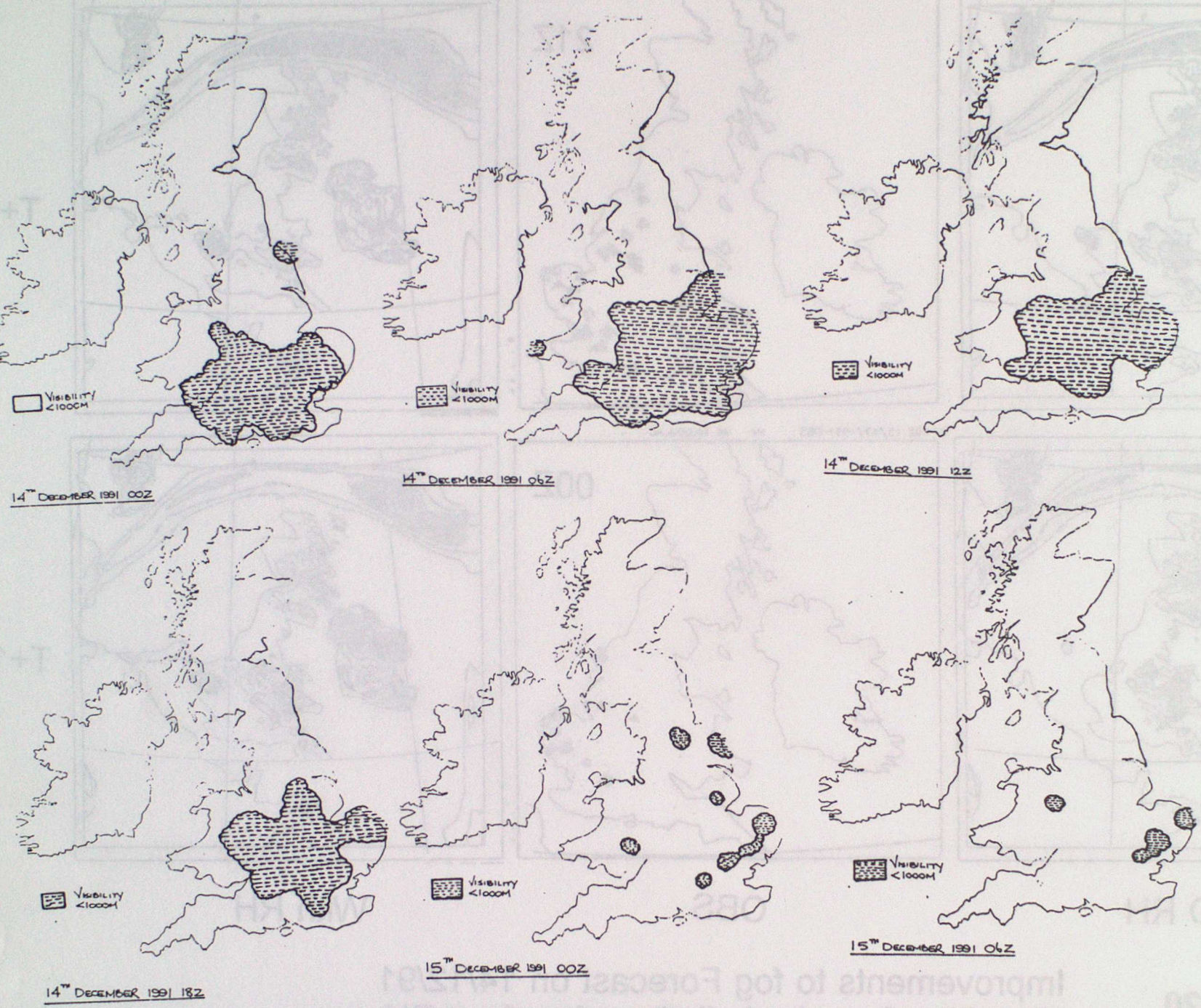

Fig. 19 Summary of fog cover from subjective interpretation of observations on 14th-15th December 1991

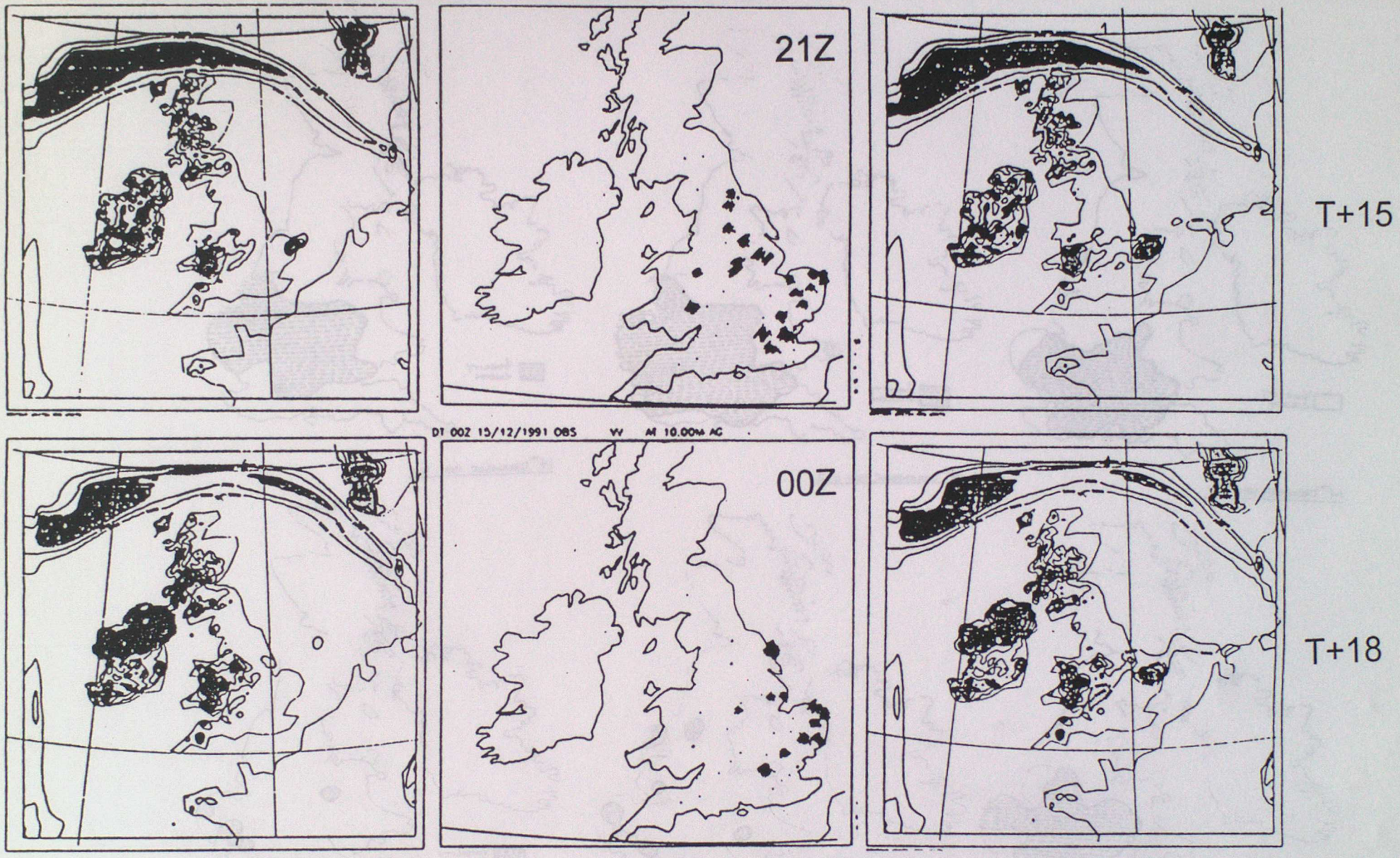

Fig. 20 Improvements to fog Forecast on 14/12/91
Resulting from Assimilation of surface RH

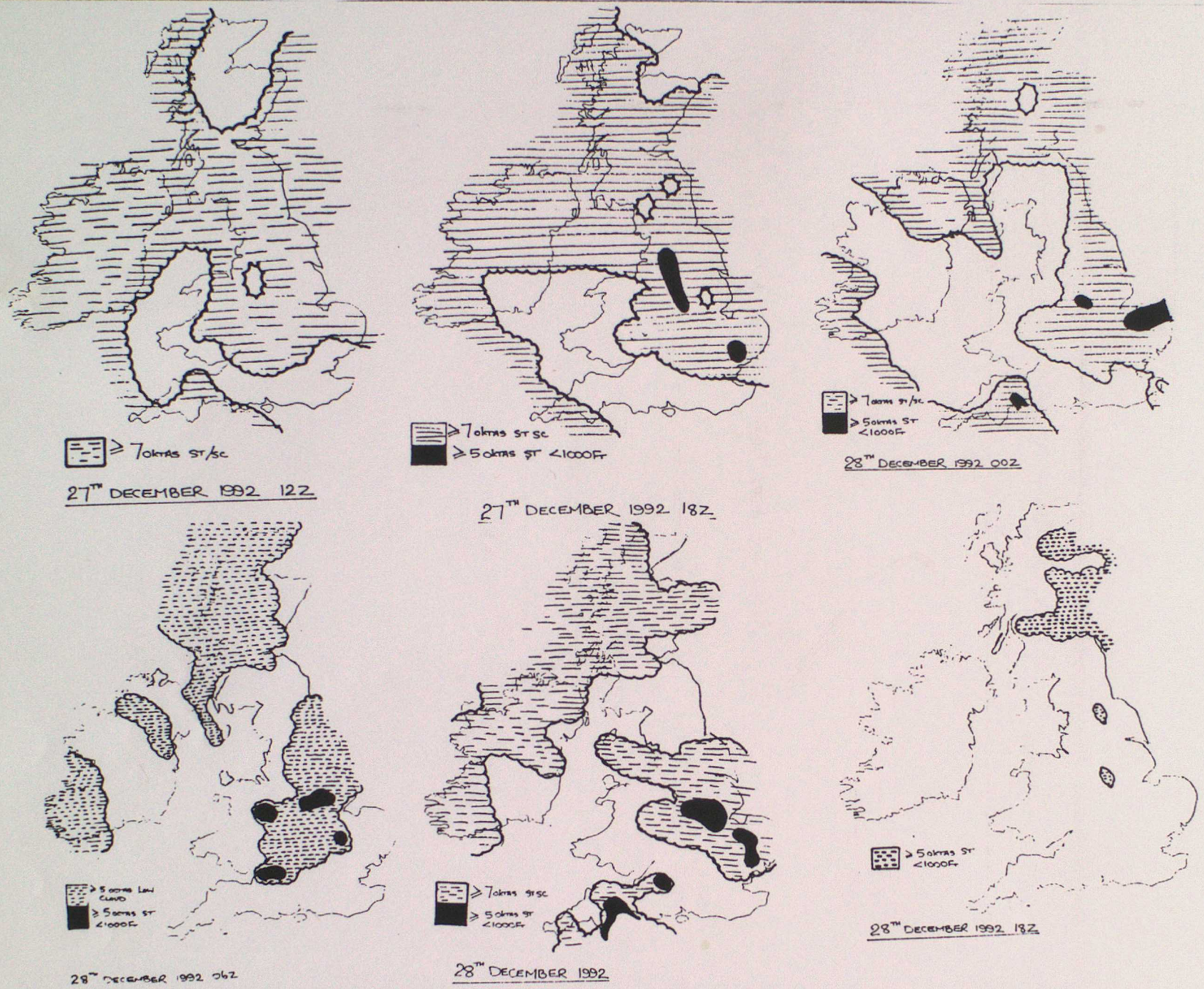

Fig. 21 Summary of fog and stratus cover from subjective interpretation of observations on 27th-28th December 1992

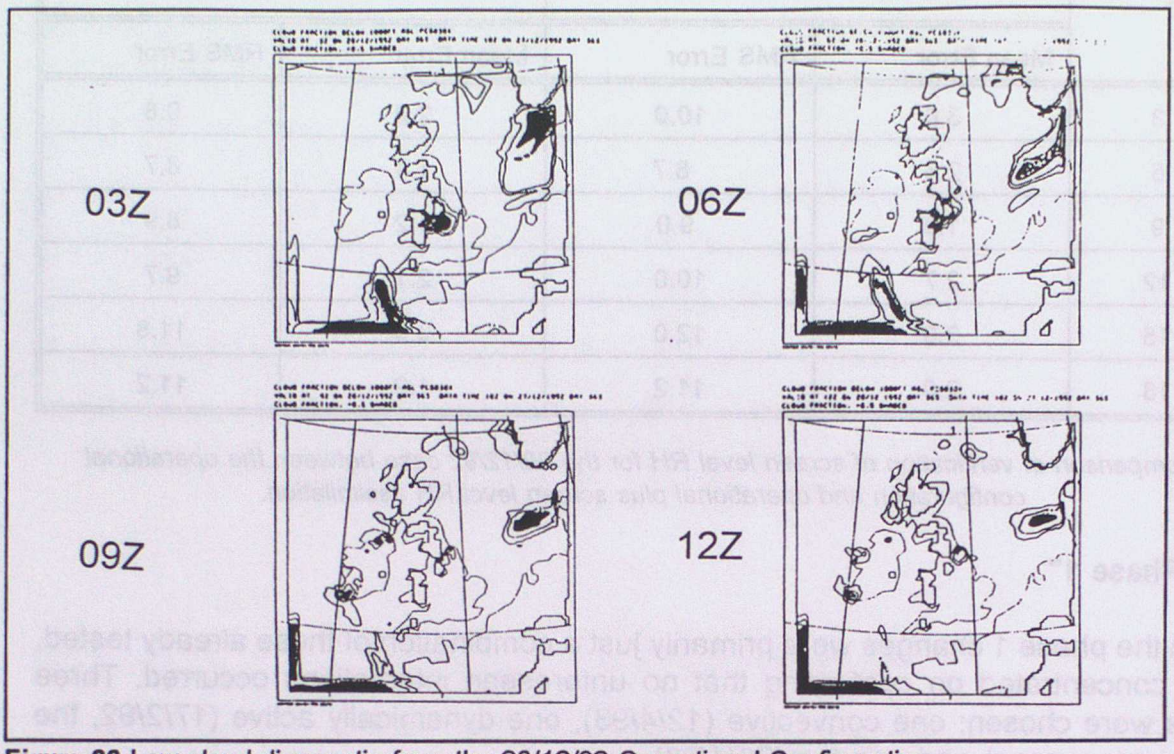

Figure 22 Low cloud diagnostic from the 28/12/92 Operational Configuration.

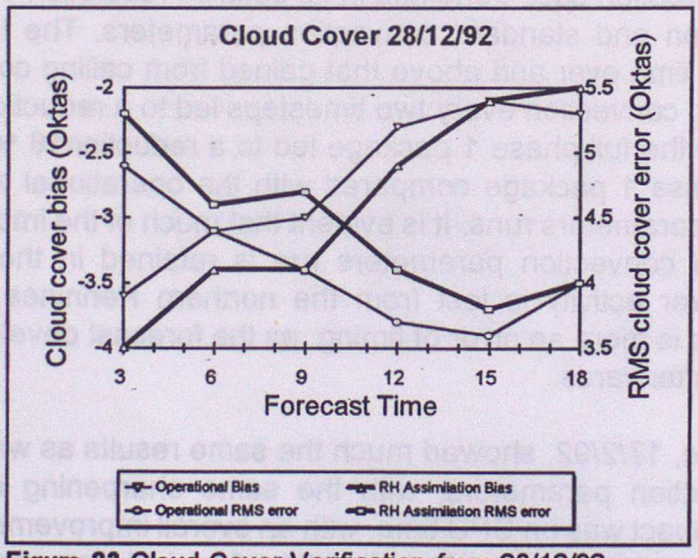

Figure 23 Cloud Cover Verification from 28/12/92.

Encouragingly, the verification of screen level RH is indeed improved throughout the forecast, though by only small amounts, as shown by the following table.

Forecast Time	Operational Run RH Error (%)		Screen RH Assimilation RH Error (%)	
	Mean Error	RMS Error	Mean Error	RMS Error
3	3.6	10.0	2.2	9.8
6	2.5	8.7	1.4	8.7
9	1.9	9.0	1.2	8.9
12	2.7	10.0	2.1	9.7
15	3.6	12.0	3.3	11.8
18	2.0	11.2	1.9	11.2

Comparison of verification of screen level RH for the 28/12/92 case between the operational configuration and operational plus screen level RH assimilation.

5.4 "Phase 1"

Since the phase 1 changes were primarily just a combination of those already tested, tests concentrated on confirming that no unforeseen interactions occurred. Three cases were chosen: one convective (12/4/93), one dynamically active (17/2/92, the frontal snow case) and one fog (30/4/93).

As expected, the convection case benefited in its detailed resolution of showers from the use of ∇^4 diffusion and standard convection parameters. The latter led to an improvement in CPU time over and above that gained from calling convection every two timesteps. Calling convection every two timesteps led to a reduction of almost 10 % in CPU time, while the full phase 1 package led to a reduction18 %. Fig. 4 shows the impact of the phase 1 package compared with the operational and the ∇^4 and standard convection parameters runs. It is evident that much of the improvement from the ∇^4 and standard convection parameters run is retained in the phase 1 run, although some shower activity is lost from the northern Pennines and Galloway peninsula. In fact, this is more an error of timing, as the forecast develops showers in these areas shortly afterwards.

The frontal snow case, 17/2/92, showed much the same results as when run with ∇^4 and standard convection parameters, with the same sharpening of precipitation features. The main impact was on CPU time, with an overall improvement of 20% over an operational configuration for a run including 6 h of assimilation and 30 h forecast.

As expected, the area where perhaps the biggest improvement in the actual forecast occurred was in fog prediction. Of particular interest was whether the revised boundary layer scheme would impact the assimilation and fog structure. In the 30/4/93 case there was very little improvement in CPU time (only 2%) but the improvement in forecast accuracy was considerable. Fig. 24 shows the fog charts corresponding to Fig. 13 from the operational configuration. The benefits arising from assimilation of surface RH were retained, with realistic fog cover resulting over central England. In fact, the extent and duration of cover were further improved, and the cover over the English Channel forecast more realistically. The fog cover appears to be well tied to

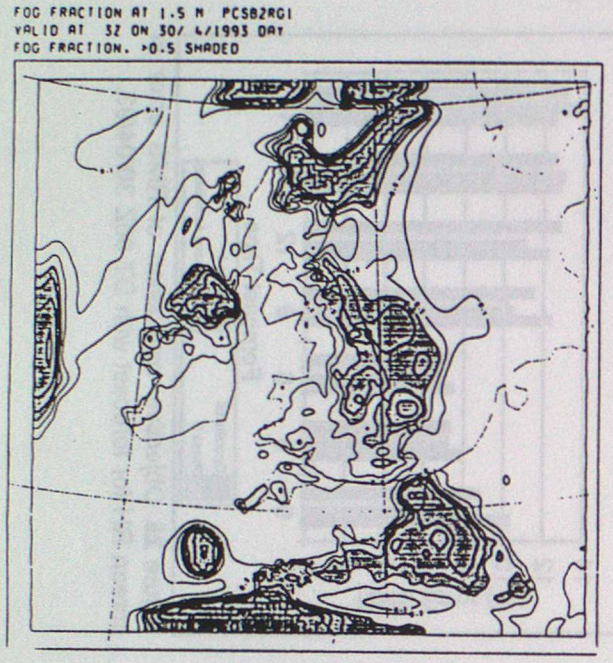

03Z

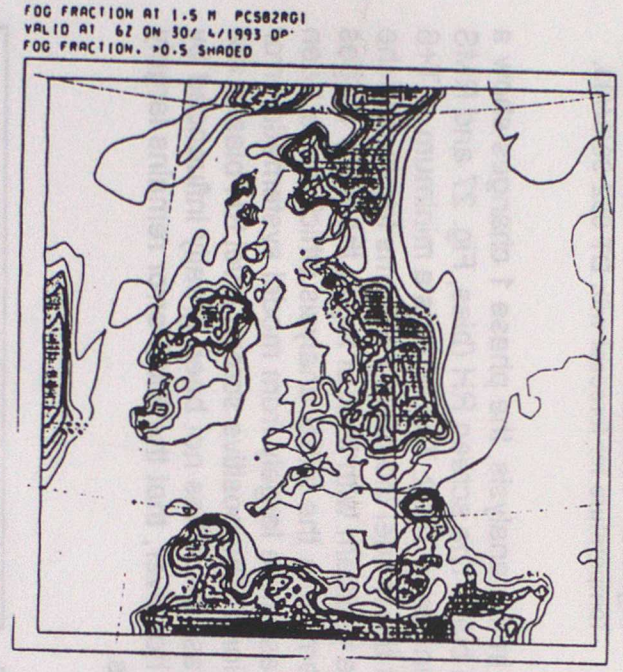

06Z

09Z

Fig. 24 00Z 30/04/93 DT Fog Probability Fields : Phase 1

orography (at least as far as it is resolved in the model), showing a very realistic gap over the North Yorkshire Moors, and burns off in very much the right fashion, although still rather too quickly. The objective verification figures for screen temperature (bias, Fig. 25 and RMS error, Fig. 26) reflect these improvements. Apart from a very small,

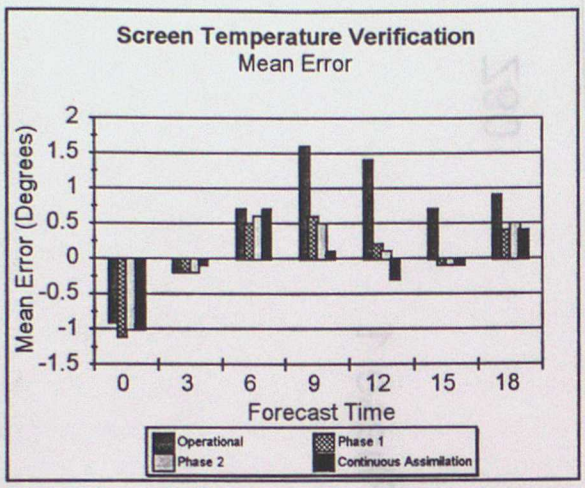

Figure 25 Verification of bias in screen temperature for forecast with DT 00Z 30/04/93.

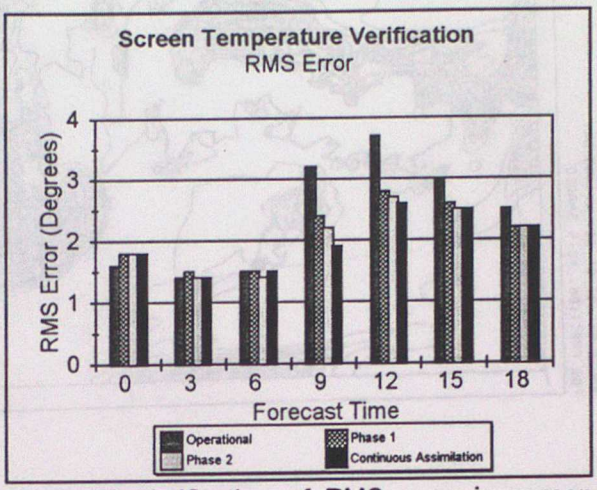

Figure 26 Verification of RMS error in screen temperature for forecast with DT 00Z 30/04/93.

and probably insignificant, deterioration in the analysis, the phase 1 changes show a considerable improvement, especially in bias. The screen RH (bias, Fig. 27 and RMS error, Fig. 28) also shows an improvement up to T+12. The error is a minimum at T+6 and the bias always positive. As a result the model incorrectly reforms fog during the early evening. It is clear that much of the problem with lack of fog in the early stages of the operational forecast arose from errors in the initial analysis which have been largely rectified. Errors later in the forecast arise largely from model systematic error and errors in the lateral boundary conditions. The positive screen level RH bias in the late afternoon is a well known model bias which has not been greatly influenced by the model changes. It should be noted, however, that the RMS error remains largely unaffected in spite of the increased bias.

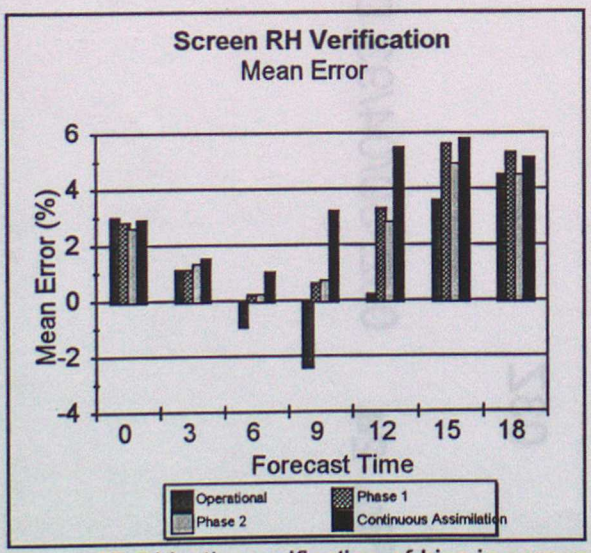

Figure 27 Objective verification of bias in screen RH for forecast with DT 00Z 30/04/93.

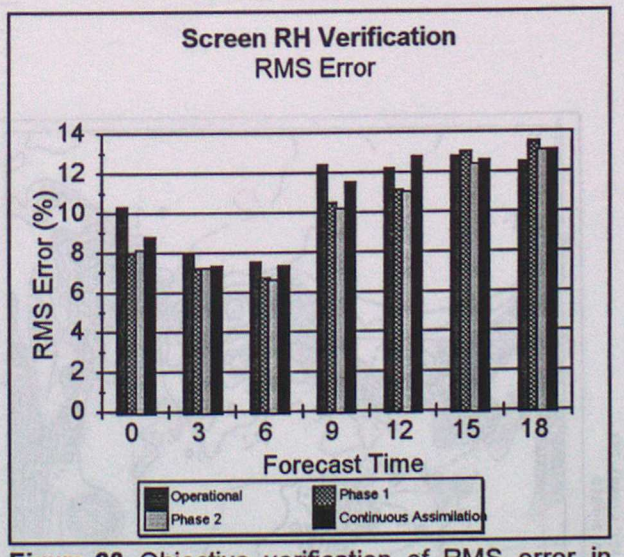

Figure 28 Objective verification of RMS error in screen RH for forecast with DT 00Z 30/04/93.

5.5 Increased vertical resolution and Revised critical RH profile

The vertical resolution of the MM is considerably less, in the boundary layer, than that of the old Mesoscale Model. In fact, the lowest level at roughly 25 m is high enough to ensure that on many occasions, thin fog may not be resolved at all. While it may be desirable to treat the surface layer in great detail, operational constraints limit the number of model levels, while consistency with the boundary layer scheme constrains how low the lowest level can be. Tests were performed using a bottom level at approximately 10 m, with some adjustment of the levels above to maintain a smooth change in level thickness. The levels are summarized in the Appendix.

The bottom few levels from the MM when first made operational are also given for comparison. Half level 6.5 is identical to the old model half level 5.5 so only levels 1 to 6 differ from original MM levels (although those above are, of course, displaced by 1). In fact, the new level 3 is only 10 m higher than the old level 2 so for many purposes may be used unchanged. Only level 2 differs markedly from the original MM, being at 40 m rather than at 25 m.

The critical RH for cloud formation should (intuitively) be related to the level thickness. As the volume of a grid box decreases to zero this should approach 100 %, but if this approach is by reduction in one dimension only it seems reasonable to suppose that the value might asymptote to a value less than 100 %. At the other extreme, the current model (and larger scale configurations) assume that higher in the model atmosphere where level thicknesses are greater the critical RH is constant (85 % at present). The current MM uses a step profile in critical RH: a constant value of 92.5 % for the bottom seven levels, and 85% above. This was chosen primarily for similarity to the LAM, where the bottom 3 levels (corresponding roughly with the bottom 7 MM levels) use a constant 92.5 %. In view of its potential importance to low cloud and fog, tests were run using a level thickness dependent formulation. Clearly, an infinite number of profiles could be chosen. To reduce the complexity of the problem, a simple profile was chosen in which the critical RH deficit from 100 % depends linearly on the level thickness and matches the constant 85 % at a specified level (8 in the MM, 9 in the MM with extra level). Thus:

$$RH_c = 1 - (1-RH_{c0}) \times (1-\beta\,(1-\delta\eta/\delta\eta_0))$$

where RH_{c0} is the critical RH at the top of the thickness dependent layer (0.85), $\delta\eta$ the (essentially pressure) thickness of the layer and $\delta\eta_0$ the thickness of the first layer with $RH_c = RH_{c0}$. The factor β is the adjustable constant which determines the slope of the profile. Thus, since level 9 is the first with RH_c=0.85, when β=1 the deficit from 1 is equal to the ratio of the level thickness to that at level 9. When β=2 the deficit from 1 is twice this. Trials have been run with β=1 and β=2, denoted RH_ca and RH_cb respectively. The two profiles are shown in Fig. 29, compared with the original. The profile β=1 was chosen for consistency with the value at level 9, to ensure a smooth function of layer thickness. Fig. 29 shows that this lies below the original curve over most of the depth of the boundary layer, and so will tend to result in a greater cloud fraction at lower RH. However, it also results in a very high value of RH_c in the bottom

layer (as it is very thin) which results in little possibility of broken cloud (or fog) in the lowest layers. The profile $\beta=2$ cures this problem, having RH_c very close to the original in level 1 (though very slightly less), with the natural result that the curve lies below the original everywhere.

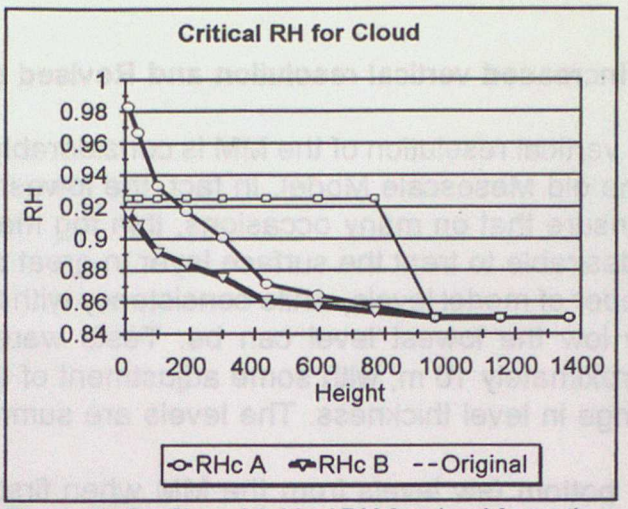

Figure 29 Profiles of Critical RH for cloud formation.

A change in the critical RH profile will have two effects. The first effect is directly on the model: a lower critical RH implies that broken cloud will form at lower RH, and so impact the radiation in the model. As a result, for example, it might be expected that radiative feedback forming fog may initiate at a lower RH. However, the second effect can act in the reverse direction: when MOPS analyses surface observations of cloud it uses observations of broken cloud to infer an RH consistent with the cloud scheme. A lower critical RH therefore means that a given cloud fraction will be analyzed as a lower RH, thereby drying the model in some circumstances.

Four cases have been run with the extra level. None have given any cause for concern regarding their numerical performance, and this has been borne out by subsequent operational experience, with no problems arising (to date) from the Phase 2 implementation. The cases chosen were all fog or stratus related, viz:

- 1st Sep 1991 Nocturnal Fog - hot day.
- 14th Dec 1991 Freezing Fog
- 28th Dec 1992 Patchy Stratus remaining from earlier fog.
- 30th April 1993 Developing Widespread Fog

The first of these was only run without assimilation as a test to see what impact the extra level has on fog formation and dissipation. In fact, in all cases, the impact on the behaviour of the model is very subtle. In most circumstances the impact is virtually undetectable. This is, in fact, to be expected and is regarded as encouraging, since in most circumstances the bottom few layers of the model are well coupled by vertical mixing so the model solution **should** be insensitive to the vertical resolution as long as the solution is numerically accurate. Only in critical conditions (primarily where a phase change is occurring or an inversion is forming) will the vertical resolution be important. The impact of the critical RH profile on the model evolution is similarly small, in fact rather less than anticipated, although there is, of course, a substantial impact on the model diagnostics concerning cloud and fog.

The impact on low cloud is illustrated by the 28/12/92 case. As already noted, this case performed badly largely because of the initial analysis. The extra level and change in RH_c did not improve the forecast considerably. However, they do have a small impact on the cloud cover verification. Examples are shown in Figs. 30 and 31, which all show a small improvement over the operational configuration, the greatest

from the RH_cb profile. The impact on the low cloud probability diagnostic is shown in Fig. 32 (next page); clearly it is not profound.

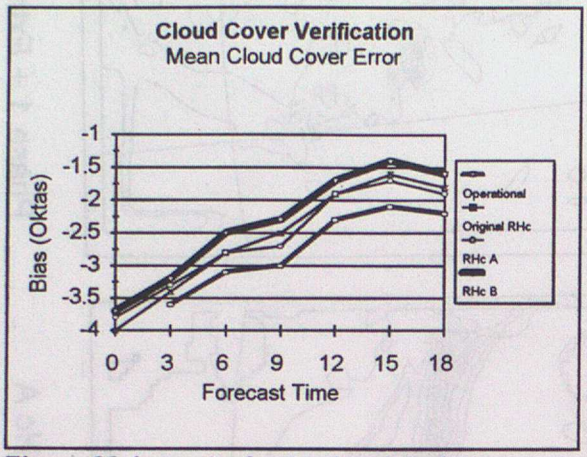

Figure 30 Impact of extra level and change in RH_c on bias in cloud cover, 28/12/92.

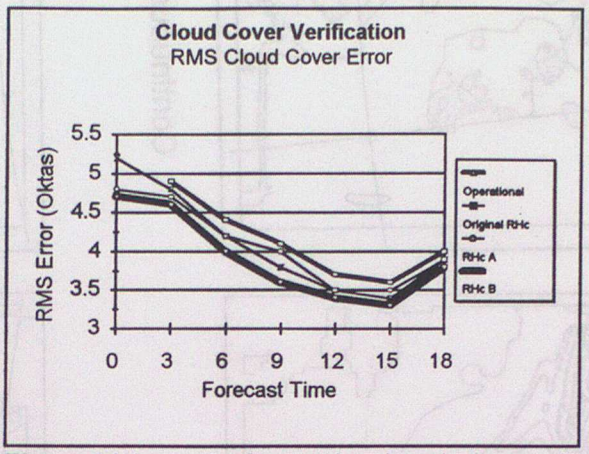

Figure 31 Impact of extra level and change in RH_c on RMS error in cloud cover, 28/12/92.

The impact on fog is a little more apparent, primarily in the fog diagnostic rather than the model evolution. The impact of the extra level and RH_cb (the 'best' of the three tested) on the 30/04/93 case is shown in the verification figures in Figs. 25 and 26 (shown as "Phase 2"). While positive, the improvement is disappointing. This rather suggests that the dissipation of the fog was determined much more by the lateral mixing of warmer, dryer air than the direct radiative warming of the fog.

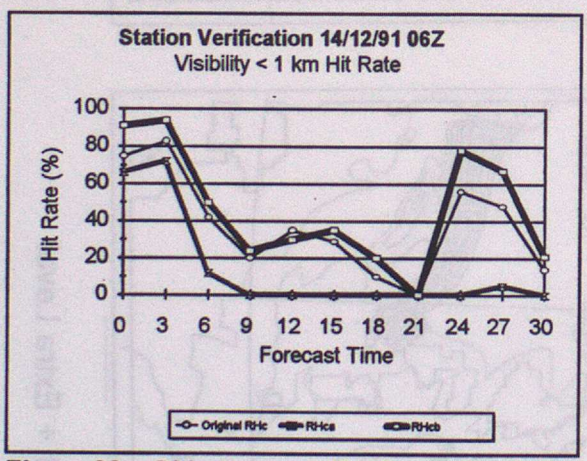

Figure 33 Objective verification of station visibility: hit rate for visibility < 1 km.

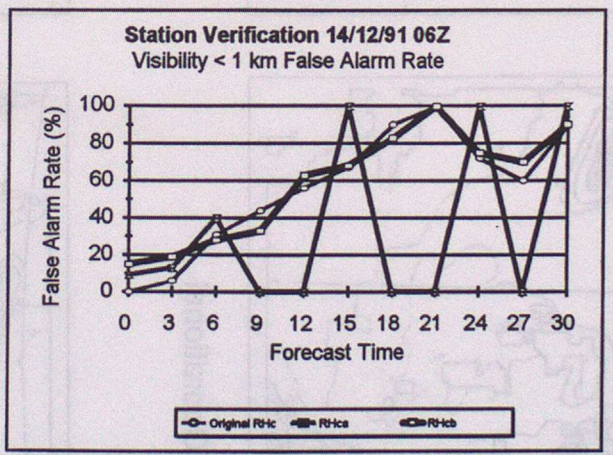

Figure 34 Objective verification of station visibility: false alarm rate for visibility < 1 km.

The station by station fog verification shows a greater impact in the 14/12/91 case (Figs. 33 and 34). As will be discussed below, this is not necessarily a very good measure of the forecast accuracy, but in this case it does give a good indication of the differences between configurations: the RH_c profile with a high value near the surface fails to reflect the patchy nature of the fog and so has a poor hit rate (and, in some cases, false alarm rate). The other two profiles show much less difference but, on the whole, the RH_cb profile shows a better hit rate with little impact on the false alarm rate.

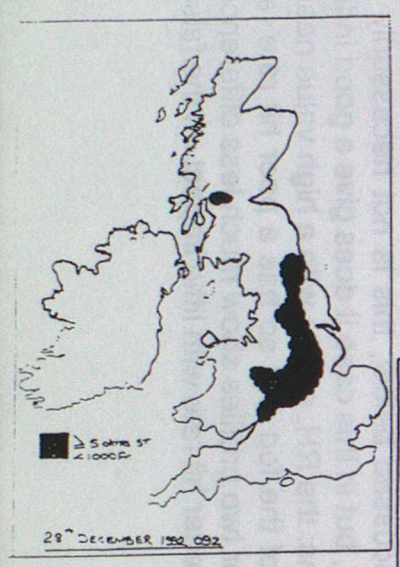

Observations

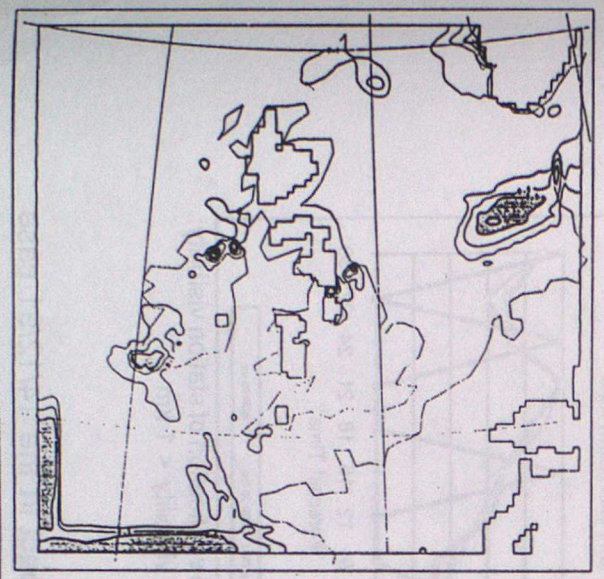

Operational

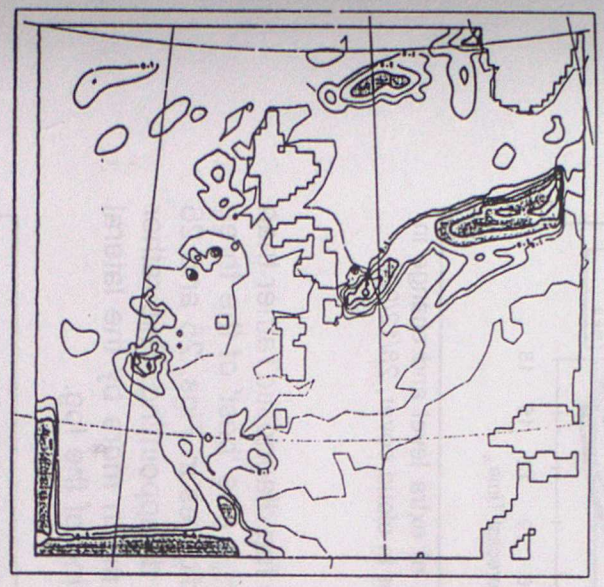

Phase 1

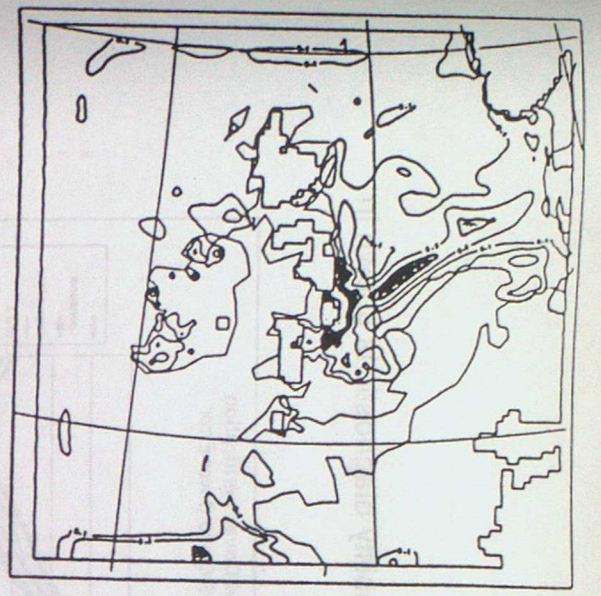

Continuous Assimilation

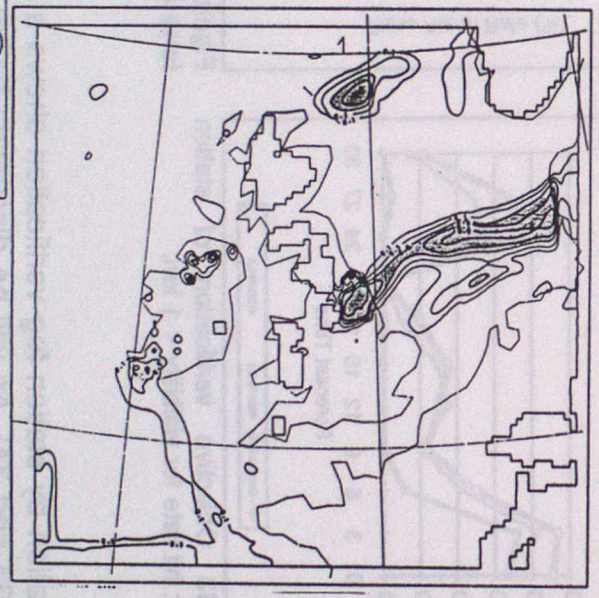

Phase 1 + Extra Level

Phase 1 + Extra Level + RHc A

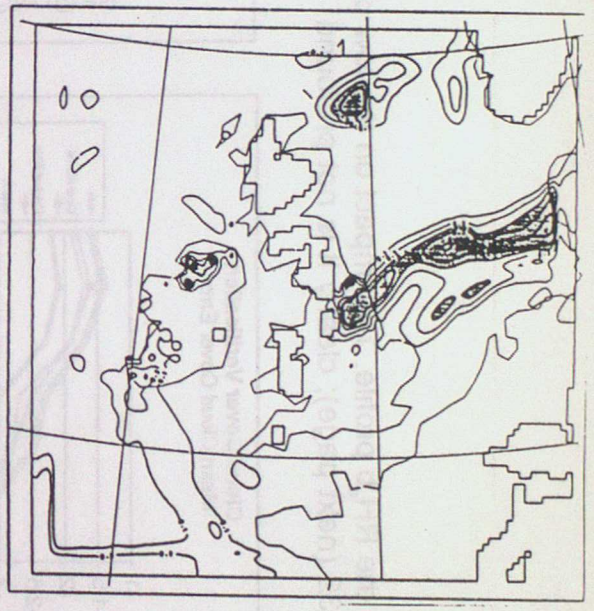

Phase 1 + Extra Level + RHc B

Fig. 32 Low cloud diagnostic at 09Z, 28th December for various model configurations, compared with subjective analysis of observations.

In summary, the higher resolution and RH_cb profile have been found to give a small improvement in forecast accuracy, and the only argument against implementing them operationally is the small increase in CPU time and storage required resulting from the higher vertical resolution. However, the improvement is not dramatic.

5.6 Automatic MOPS

The MM Moisture Observation Preprocessing System (MOPS) developed out of the OMM Interactive Mesoscale Initialization (IMI), and relied on forecaster intervention to correct gross errors in cloud top height and cover, which were particularly likely when the inversion associated with the top of a stratocumulus sheet was poorly resolved in the model. This system has been replaced with a fully automated system which uses new algorithms. AutoMOPS is a substantial system in its own right and is being reported fully elsewhere (Wright, 1994). Trial results will not be considered here beyond saying that the objective of freeing forecaster resources without degrading the analysis was fully met. Although the analysis may be different from that produced interactively, the impact on the forecast is small and generally beneficial. The system has been operational since October 1993 without any noticeable degradation in the operational forecasts.

5.7 Continuous Assimilation and Four runs a day

The current operational procedure comprises two 3 hour assimilation cycles followed by a forecast (18 h for the 00Z run and 30 h for the 06Z run). The 00Z and 06Z systems are entirely independent, both starting from larger scale initial fields (the LAM in the case of 00Z and the global analysis in the case of 06Z). The whole process is illustrated in Fig. 35. As illustrated above, many of the errors that arise in forecasts result from the initial analysis, which, of course, is greatly influenced by the initial field at the start of the data assimilation period. Aspects involving the boundary layer and/or topography will particularly suffer, as these are poorly resolved in the larger scale models. These aspects include fog and low cloud.

A continuous assimilation system was proposed with fog and low cloud particularly in mind. The system is illustrated in Fig. 36. The two short forecasts followed by the full forecast required for both the 00Z and 06Z run are replaced by a continuous sequence of 3 hours of assimilation from the previous analysis (to give an analysis) followed by 3 hours forecast to give first guess fields for observation quality control and MOPS analysis. Any of these may be continued to give a longer forecast: the proposal was made to use the following sequence:

00Z to T+18 (18Z)
06Z to T+30 (12Z next day)
12Z to T+24 (12Z next day)
18Z to T+18 (12Z next day)

Two aspects of the system were thus tested, the first being the improvement in analysis and forecast arising from continuous assimilation, the second being the ability of the new forecasts (12Z and 18Z) to give earlier warning of night time fog and subsequent clearance.

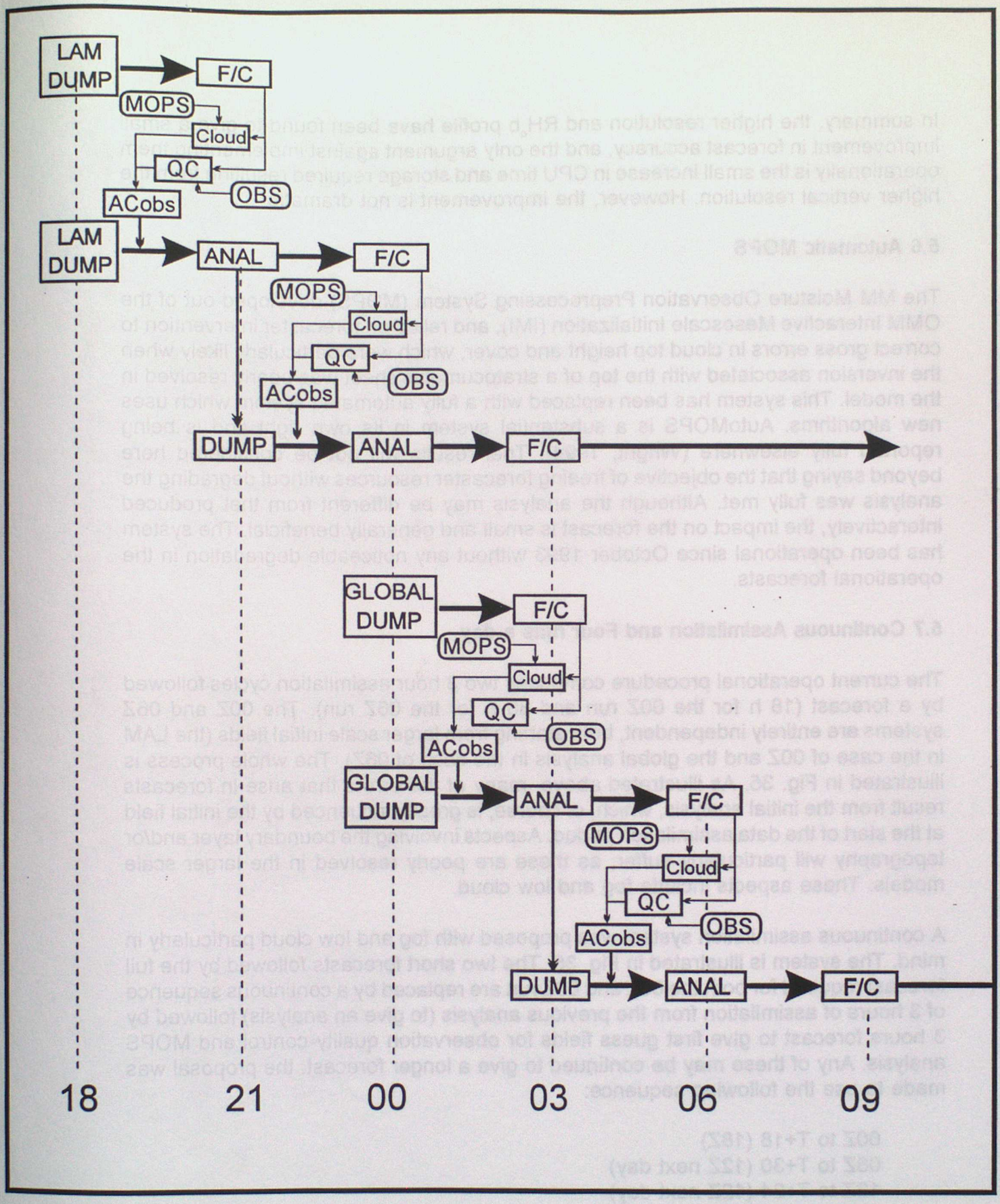

Fig. 35 Schematic representation of current operational schedule for mesoscale model runs.

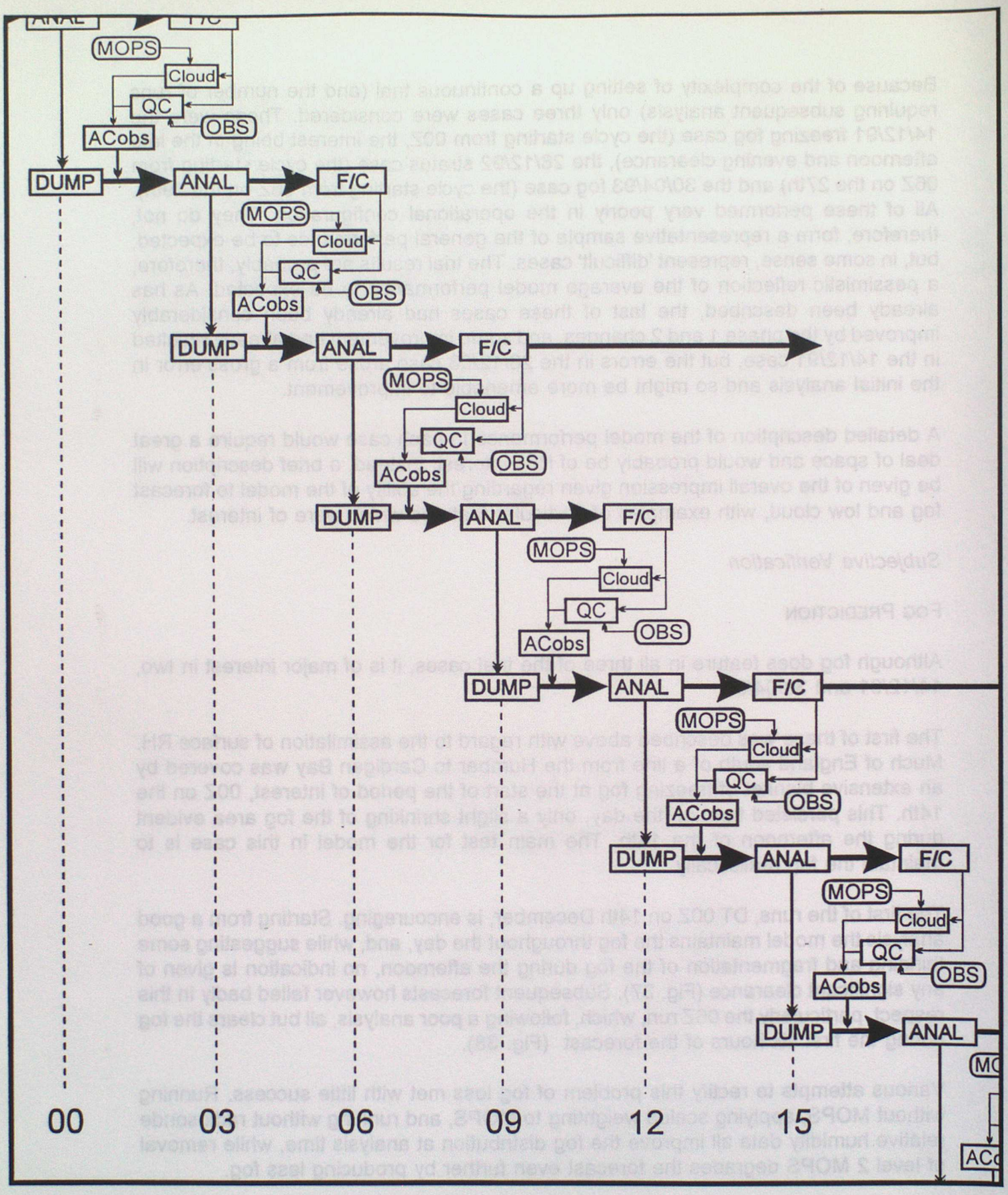

Fig. 36 Schematic representation of part of the continuous assimilation schedule for mesoscale model runs.

Because of the complexity of setting up a continuous trial (and the number of runs requiring subsequent analysis) only three cases were considered. These were the 14/12/91 freezing fog case (the cycle starting from 00Z, the interest being in the late afternoon and evening clearance), the 28/12/92 stratus case (the cycle starting from 06Z on the 27th) and the 30/04/93 fog case (the cycle starting from 06Z on the 29th). All of these performed very poorly in the operational configuration. They do not, therefore, form a representative sample of the general performance to be expected, but, in some sense, represent 'difficult' cases. The trial results are probably, therefore, a pessimistic reflection of the average model performance to be expected. As has already been described, the last of these cases had already been considerably improved by the phase 1 and 2 changes, and some improvement had already resulted in the 14/12/91 case, but the errors in the 28/12/93 case arose from a gross error in the initial analysis and so might be more amenable to improvement.

A detailed description of the model performance in each case would require a great deal of space and would probably be of little interest. Instead, a brief description will be given of the overall impression given regarding the ability of the model to forecast fog and low cloud, with examples of particular features which were of interest.

Subjective Verification

FOG PREDICTION

Although fog does feature in all three of the trial cases, it is of major interest in two, 14/12/91 and 30/04/93.

The first of these was described above with regard to the assimilation of surface RH. Much of England south of a line from the Humber to Cardigan Bay was covered by an extensive blanket of freezing fog at the start of the period of interest, 00Z on the 14th. This persisted through the day, only a slight shrinking of the fog area evident during the afternoon of the 14th. The main test for the model in this case is to maintain the fog realistically.

The first of the runs, DT 00Z on 14th December, is encouraging. Starting from a good analysis the model maintains the fog throughout the day, and, while suggesting some thinning and fragmentation of the fog during the afternoon, no indication is given of any significant clearance (Fig. 37). Subsequent forecasts however failed badly in this respect, particularly the 06Z run, which, following a poor analysis, all but clears the fog during the first six hours of the forecast (Fig. 38).

Various attempts to rectify this problem of fog loss met with little success. Running without MOPS, applying scaled weighting to MOPS, and running without radiosonde relative humidity data all improve the fog distribution at analysis time, while removal of level 2 MOPS degrades the forecast even further by producing less fog.

The largest impact at analysis time was evident with the 'no MOPS' run, and Fig. 39 shows a comparison of this run with the standard version. This run corresponds in data time to that used in earlier trials and so may be compared directly. The comparison is generally unfavourable. The initial analysis and the subsequent

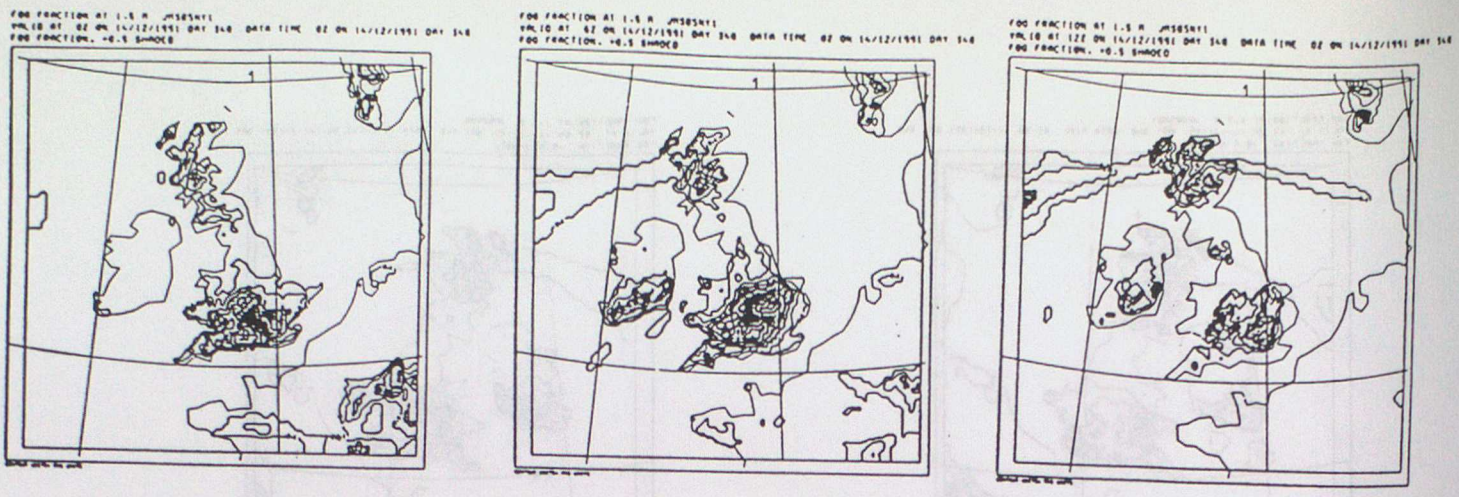

00Z 06Z 12Z

Fig. 37 Fog probability forecasts from 00Z to 12Z, 14/12/91, from continuous assimilation run with DT 00Z.

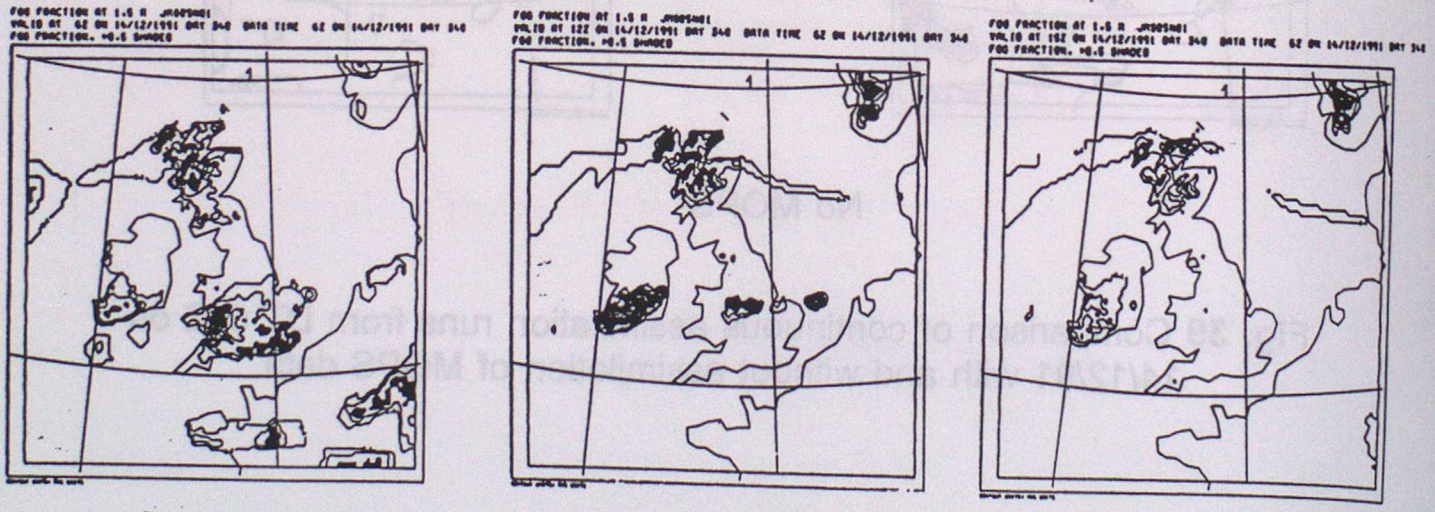

06Z 12Z 15Z

Fig. 38 Fog probability forecasts from 06Z to 15Z, 14/12/91, from continuous assimilation run with DT 06Z.

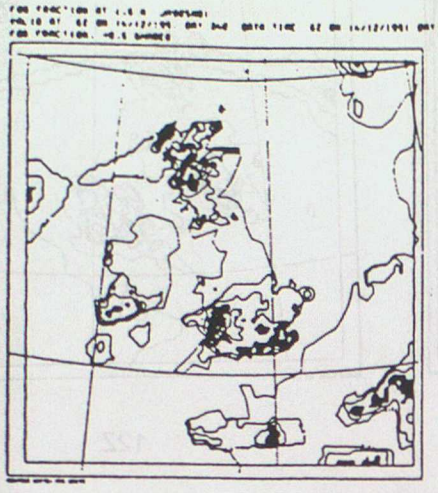

06Z

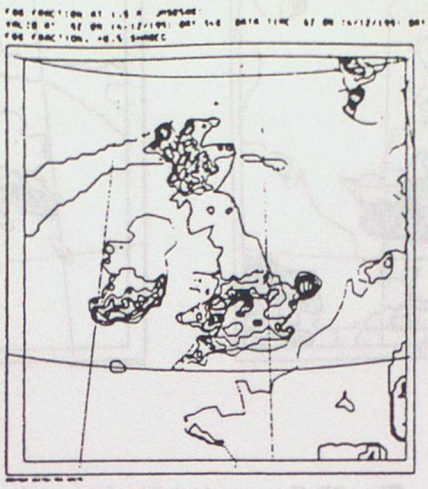

Standard

09Z

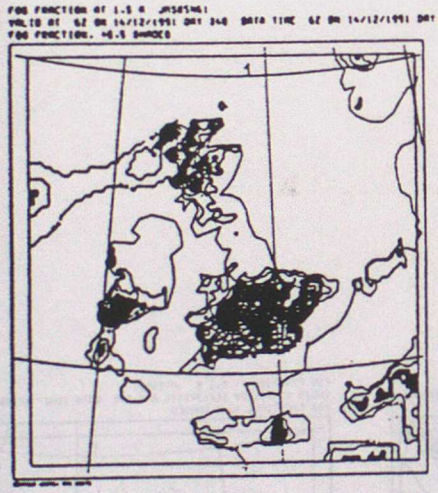

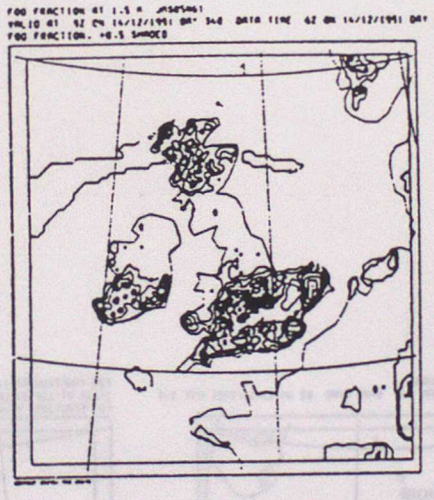

No MOPS

Fig. 39 Comparison of continuous assimilation runs from DT 06Z on 14/12/91 with and without assimilation of MOPS data.

Fig. 40 Comparison of fog probability results from continuous assimilation runs with successive data times, for 03-09Z 30/04/93.

development are both worse. This suggests that the initial field used from the continuous assimilation cycle up to 06Z (which only started at 18Z) is worse than that from the assimilation cycle started at 00Z from a global analysis.

During the late evening of 14th December the fog largely cleared, although with some patches persisting, notably over East Anglia. Model success in representing this is variable. Overall the tendency is for the model to reform fog during the evening, and this is overdone, especially in the 12Z run. The 18Z run however, although starting from a poor analysis, does suggest more realistically the patchy nature of the fog.

The second of the fog cases, 30/04/93, is considerably more successful. The main period of interest is the period of fog formation and dissipation from 03Z to 12Z. Fog forecast results are summarized in fig. 40, which should be compared with Figs. 8 and 9. Guidance on the deteriorating visibility overnight on 29th/30th is available from the first of the runs, 06Z on 29th April, with generally increasing detail on fog formation added on subsequent runs. The one exception to an otherwise good sequence of forecasts, however, is the 12Z run on the 29th. This run is indifferent early in the forecast period, and gives little indication of deteriorating visibility during the following night. Various reruns of this particular forecast were carried out as follows:

(1) Extra weighting to MOPS
(2) No radiosonde relative humidity data
(3) No MOPS
(4) Run using boundary conditions from 06Z LAM

Unfortunately none of these reruns go any way towards improving the fog representation, although by the following run, 18Z on the 29th, model advice is once more reasonable, and a good indication is given of the thickest fog in eastern England later in the night. This run, however, does look deficient in fog production in south and southwest England, although by the following run at 00Z this error seems to have been largely rectified.

One point may be of value in interpreting the fog probability charts in future. It is evident, in particular from the 00Z run, that the model appears, realistically, to be differentiating (in terms of fog probability) between the thicker fog in the east, and what the observations suggest is thinner and probably more patchy fog further west.

The guidance on fog clearance is reasonable. Although the 18Z forecast clears the fog rather too quickly, subsequent runs do provide generally good advice.

Low Cloud Prediction

Two of the trial cases feature low cloud, 30/04/93 and 28/1/92. In the April case, a fairly extensive area of low stratus covered England at the start of the period of interest, 06Z on 29th April, clearing gradually during the morning. Model guidance on this feature is a little questionable. The 06Z run on the 29th does give some indication of this cloud, but looks deficient at analysis time and then goes on to clear the cloud too quickly (figure 41). On a more positive note, this case does feature an area of low

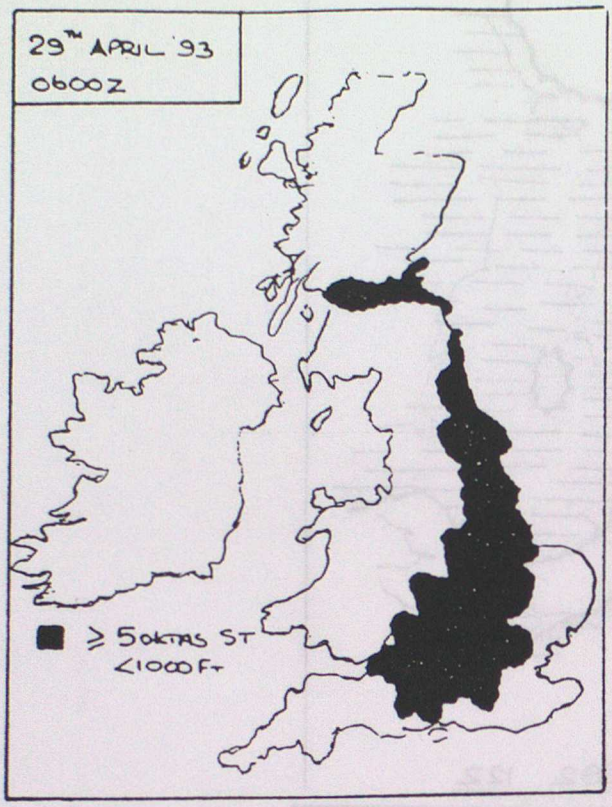

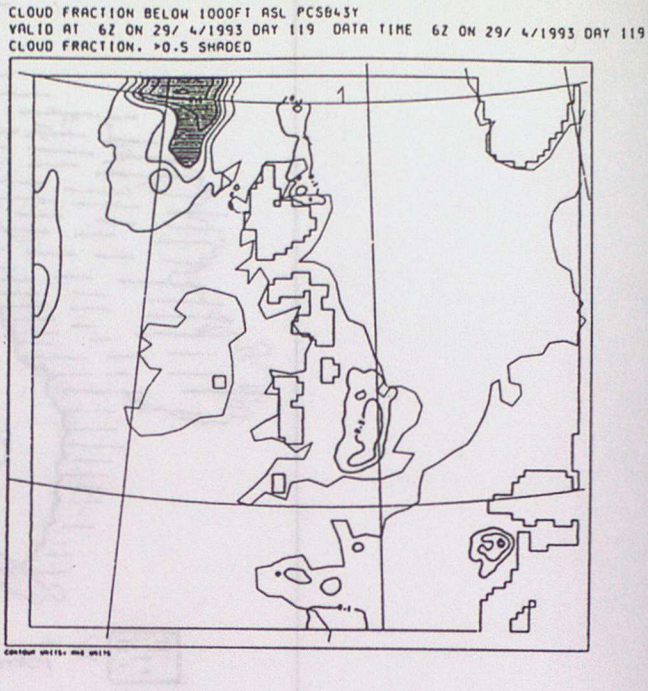

06Z

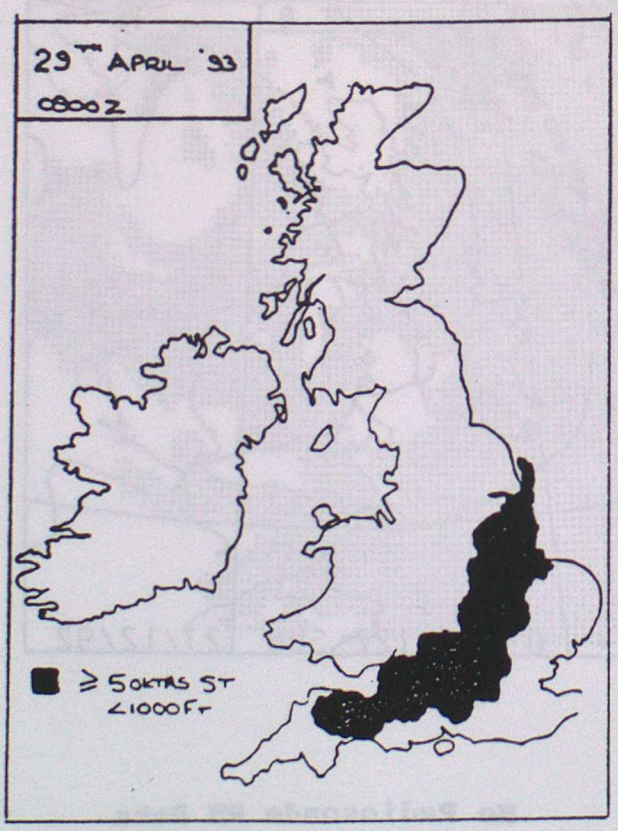

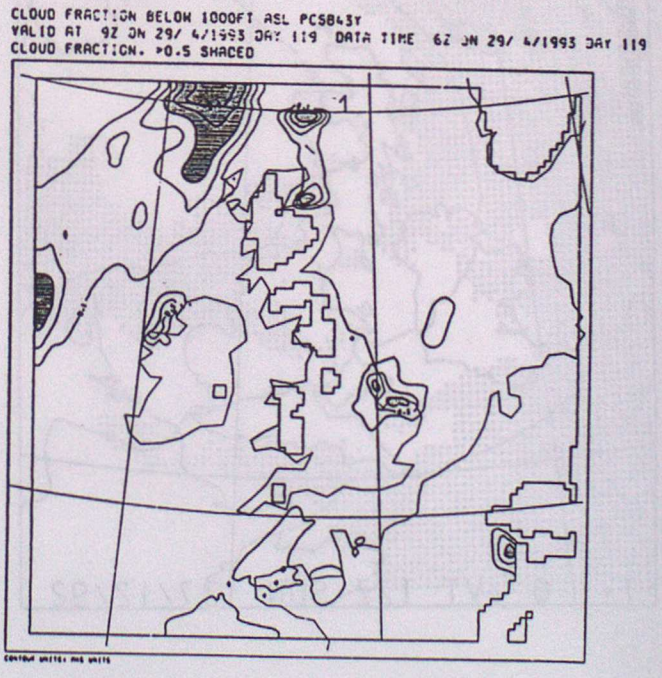

09Z

Fig. 41 Low cloud from the 06Z continuous assimilation run on 29/4/93 compared with observations.

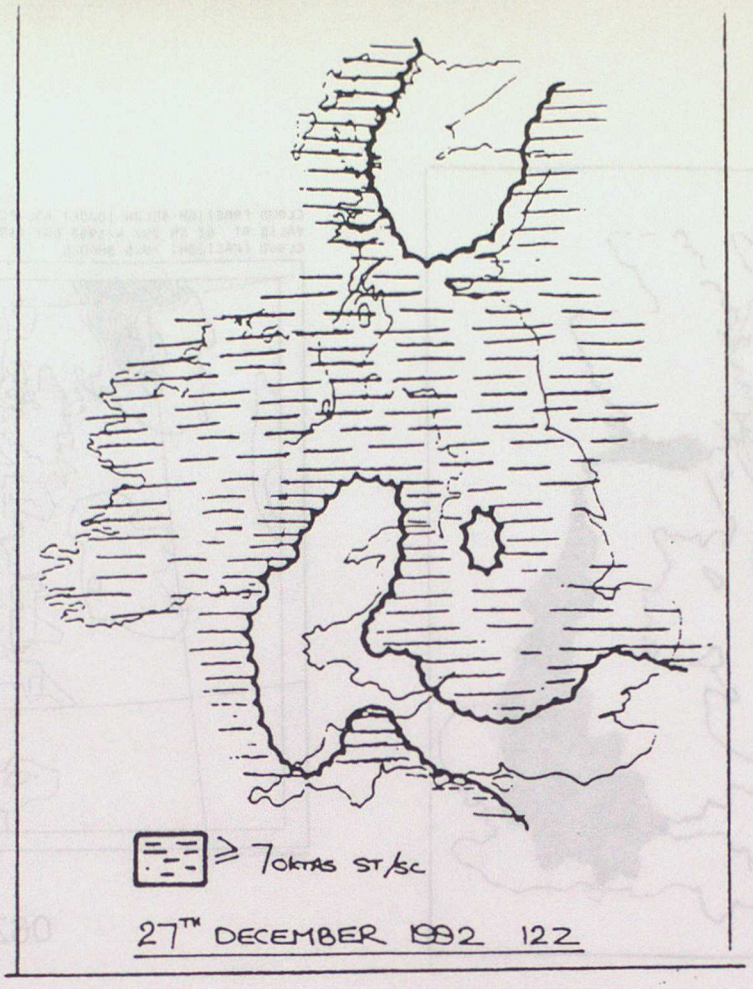

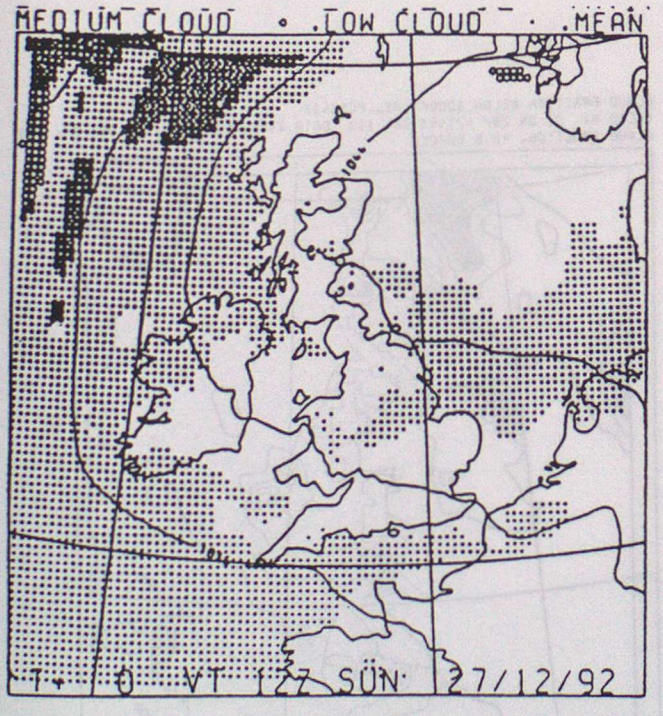

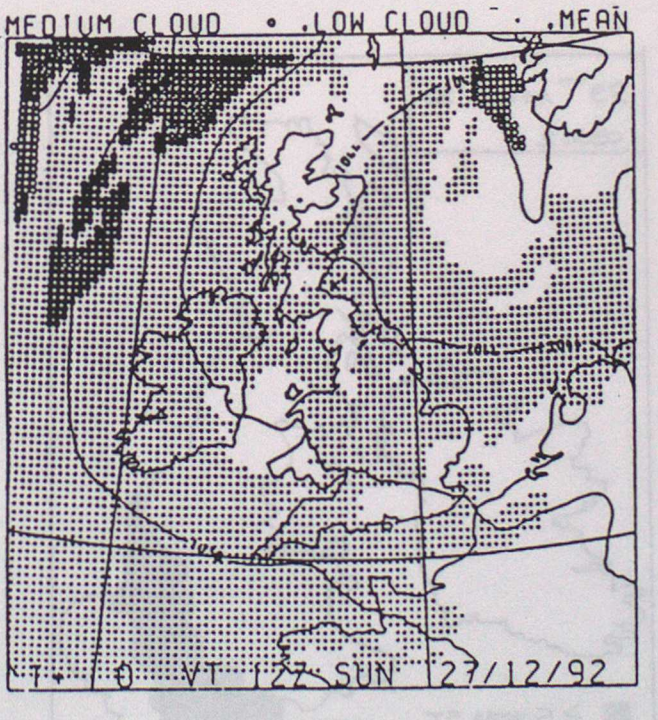

Standard

No Radiosonde RH Data

Fig. 42 Comparison of analysis cloud charts in continuous assimilation runs at 12Z 27/12/92, with and without assimilation of radiosonde data.

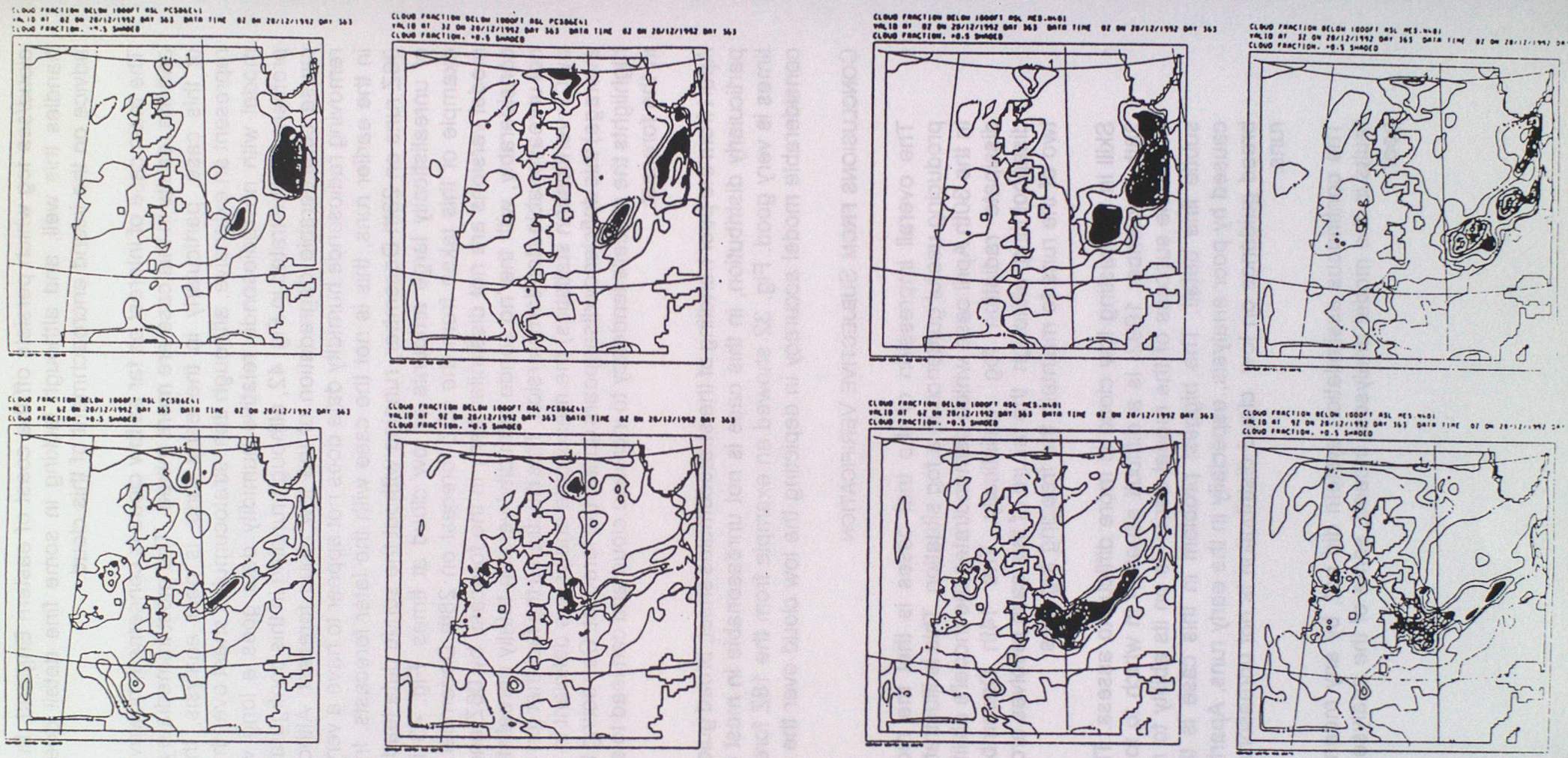

Cloud Fraction below 1000ft

Cloud Fraction below 1000ft
No Radiosonde RH Data

Fig. 43 Comparison of low cloud charts in continuous assimilation runs from 00Z 28/12/92, with and without assimilation of radiosonde data.

cloud/sea fog which persists off the coast of eastern England. In general the model handles this well, and although lacking in some fine detail does give reasonable advice on the inland encroachment of this cloud.

The main case of interest as far as low cloud is concerned, however, is the 28/12/92, and the results in this case are more mixed. The most immediate and striking feature of this case, particularly in the early runs, is poor analysis, the model failing to represent an extensive, although thin, stratocumulus sheet over the UK. Running the model with no radiosonde relative humidity data goes a long way to solving this problem, as illustrated in Fig. 42, although running in this configuration does, at times, cause considerable degradation of the low cloud forecast. Although the impact of removing radiosonde humidity data does not appear to have a very significant impact in the earlier runs, this is not the case with the later forecasts. In both the 00Z and 06Z runs on 28th December, running without the sonde data leads to the production of unrealistically large amounts of low cloud at times. Fig. 43 illustrates a typical example of this taken from the 00Z forecast on 28th December. Although the two model versions are not dissimilar early in the forecast, by 06Z and 09Z they diverge considerably, with the 'no sonde humidity' version totally unrealistic compared to the not unreasonable standard version. This illustrates the fact that (on average, illustrated by CF verification statistics) the mesoscale analysis is deficient in cloud, and that (on average) this deficiency disappears during the forecast. Correcting the initial cloud bias highlights the model's tendency to increase cloud and can lead to a poorer result later in the forecast.

Apart from the poor handling of the stratocumulus sheet, broad guidance on low cloud, particularly distribution, in this case is not unreasonable in most of the runs, and at times is very good. Fig. 32 showed an example from the 18Z forecast and indicates considerable model accuracy in depicting the low cloud over the Pennines.

Conclusions from Subjective Verification

- The overall impression of the trial cases is that the model is capable of producing useful guidance in a fog situation. This is illustrated particularly well in the 30th April case which demonstrates the model's ability both to form and dissipate radiation fog realistically. The 14th December case is more disappointing, although the failure of this case revolves around the inability of two of the runs to maintain the freezing fog area.

- Skill in forecasting low cloud is more difficult to assess. The main trial case, 28th December 1992, is a difficult situation in which to forecast, and one in which the success of the model depends on its ability to resolve some fairly subtle fine detail. The biggest problem in this case is the low confidence caused by poor analysis, especially in the early runs. Apart from this however broad guidance on low cloud distribution is not unreasonable in most of the runs.

- The continuous assimilation system did not, by any means, rectify all of the faults in the model analyses. Indeed, some of the analyses were remarkably poor.

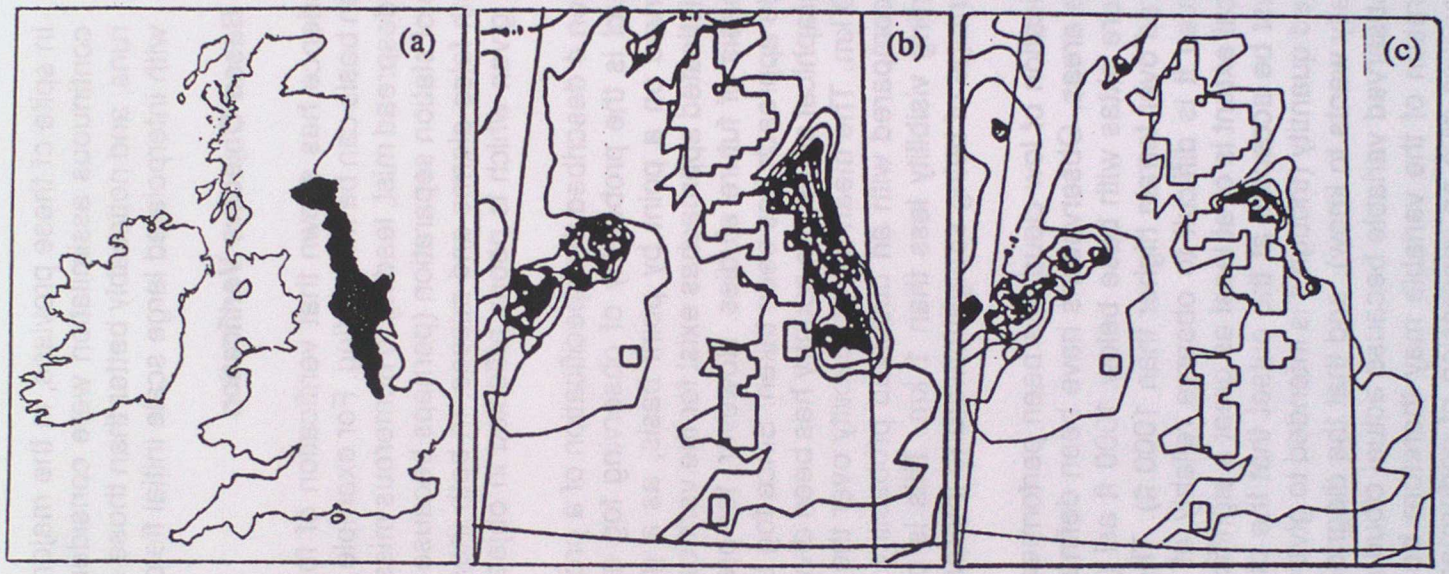

Fig. 44

(a) Observations at 00z 30/4/93, >4 oktas cloud <1000ft shaded.
(b) t+6 cloud fraction below 1000ft above sea level (>50% shaded) from CONTINUOUS assimilation run, DT 18z 29/4/93.
(c) as (b) but with INTERMITTENT assimilation.

- In some cases, the model appeared to introduce correctly features as the forecast progressed which had been absent from the analysis, thereby improving the verification. This points towards some problems with the assimilation system which have yet to be fully resolved together with errors in the model which, in this case, compensate for the analysis errors as the forecast progresses.

- In spite of these provisos, in the majority of cases the forecasts resulting from continuous assimilation were considerably better than equivalent operational runs, and noticeably better than those run using phase 1 and phase 2 changes with interpolated large scale initial fields. A good example is shown in Fig. 44.

Area Based Objective Verification

Experience has shown that verification of fog and stratus forecasts on a station by station basis can be misleading. For example, isolated patches of fog may be forecast as widespread mist, leading to numerous misses, or patches located incorrectly on the scale of station separation (perhaps because of smoothed model orography), leading to both false alarms and misses. In both these examples useful guidance may have been given which is poorly reflected in objective verification figures.

Section 4 described the specification of a probabilistic fog diagnostic. The diagnosed product is the probability of observing fog at a given point. This cannot be directly observed on a point by point basis, as a given point is either foggy or not. More sophisticated approaches exist for the verification of such probabilities which will form the basis of future studies. However, for present purposes a rather pragmatic and simple approach has been taken. Since fog tends to occur associated with particular geographical areas, the country has been divided into a number of areas, of order 100 x 100 km. The mean fog probability over the area is derived from the model product and compared with an observed probability derived from the proportion of stations reporting visibility less than 1 km. This is clearly a crude verification, but has the advantage of being straightforward to interpret.

Verification of low cloud has been performed very similarly by aggregating over the same areas. Observations have been defined as showing low cloud if they report 3 or more oktas with base below 1000 ft asl (clearly, observations and forecasts are ignored over terrain higher than 1000 ft). The actual cloud amount is ignored, partly because it is difficult to observe reliably at such low level and partly because the vertical extent is of at least as great a significance but impossible to observe reliably. It must be accepted at the outset that the diagnostic is not exactly the same as the verified quantity (though it is intended to give a realistic indication of what a forecaster actually wants to know), and that the diagnostic is likely to give a smaller value than the observed variable because actual cloud amount above 2 oktas is ignored. Some calibration of the variable may therefore be required.On the whole the area based diagnostics give an impression of performance similar to a subjective assessment, unlike, at times, station by station based statistics.

The geographical areas used are shown in Fig. 45. For the purposes of verification the upland areas were not included: only areas 1, 2, 3, 4, 6, 9, B, C and D were used.

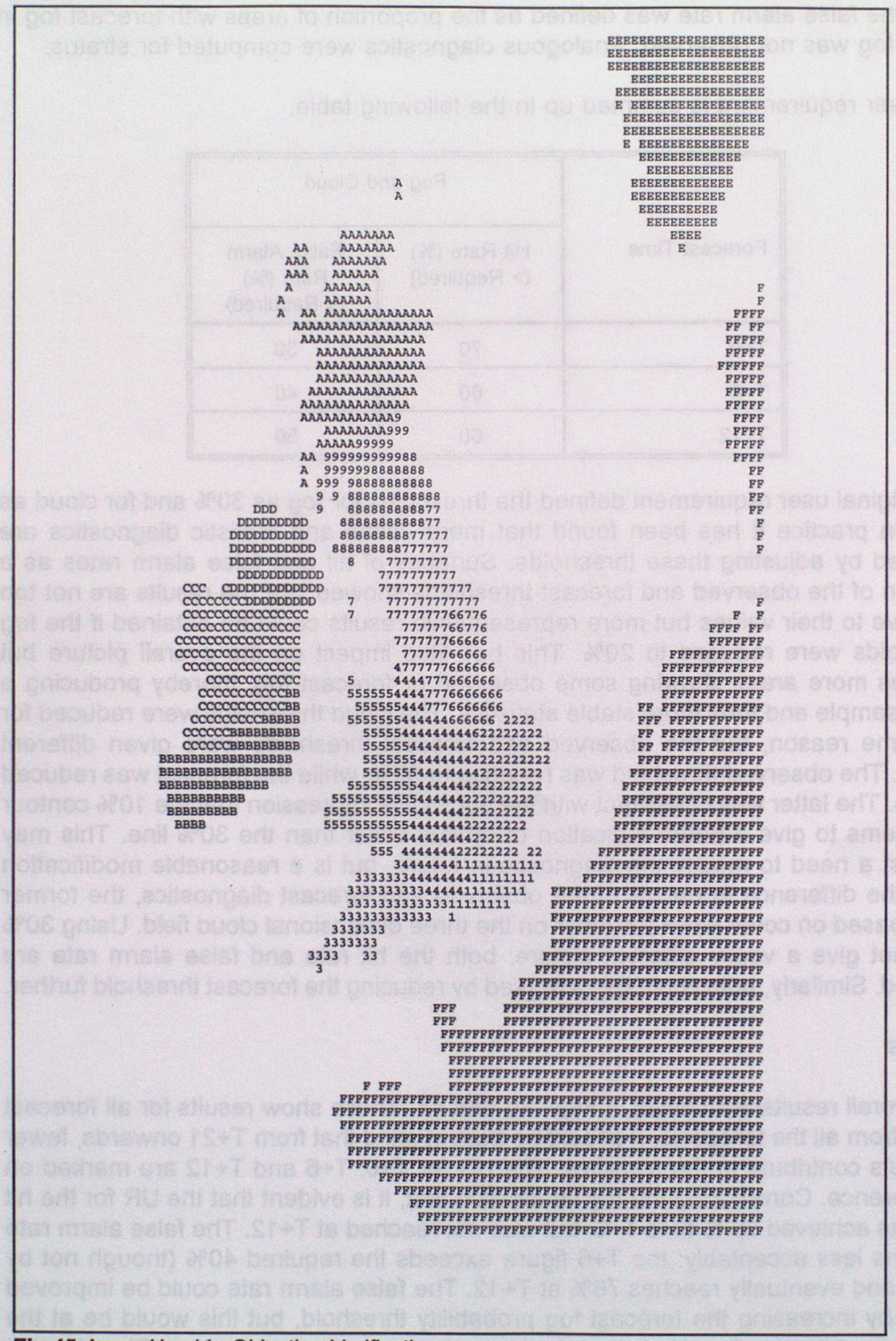

Fig.45 Areas Used in Objective Verification

The user requirement (UR) was defined using the achieved hit rate and false alarm rate for these areas. An area was defined as being observed or forecast as foggy if the observed or forecast fog probability exceeded a certain threshold. The hit rate was defined as the proportion of areas with observed fog which were successfully forecast, while the false alarm rate was defined as the proportion of areas with forecast fog in which fog was not observed. Analogous diagnostics were computed for stratus.

The user requirement is summed up in the following table.

Forecast Time	Fog and Cloud	
	Hit Rate (%) (> Required)	False Alarm Rate (%) (< Required)
T+0	70	30
T+6	60	40
T+12	60	50

The original user requirement defined the thresholds for fog as 30% and for cloud as 50%. In practice it has been found that more useful and realistic diagnostics are obtained by adjusting these thresholds. Surfaces of hit and false alarm rates as a function of the observed and forecast thresholds showed that the results are not too sensitive to their values but more representative results could be obtained if the fog thresholds were reduced to 20%. This has little impact on the overall picture but includes more areas showing some observed or forecast fog, thereby producing a larger sample and thus more stable statistics. The cloud thresholds were reduced for the same reason, but the observed and forecast thresholds were given different values. The observed threshold was reduced to 30%, while the forecast was reduced to 10%. The latter was consistent with the subjective impression that the 10% contour line seems to give a better indication of stratus cover than the 30% line. This may suggest a need to modify the diagnostic in future, but is a reasonable modification given the difference in nature of the observed and forecast diagnostics, the former being based on cover while the latter on the three dimensional cloud field. Using 30% does not give a vastly different picture: both the hit rate and false alarm rate are reduced. Similarly, both could be increased by reducing the forecast threshold further.

Results

The overall results are shown in Figs. 46 and 47. These show results for all forecast times, from all the forecasts. It should be born in mind that from T+21 onwards, fewer forecasts contribute to the statistics. The UR for T+0, T+6 and T+12 are marked on for reference. Considering the fog verification first, it is evident that the UR for the hit rate was achieved up to time T+6, but was not reached at T+12. The false alarm rate performs less acceptably: the T+6 figure exceeds the required 40% (though not by much) and eventually reaches 76% at T+12. The false alarm rate could be improved simply by increasing the forecast fog probability threshold, but this would be at the cost of the hit rate. Overall, however, the performance is encouraging. The shortfall

in performance is not extremely large and might be accounted for by an unfavourable choice of cases.

The low cloud performance is disappointing in that the user requirement is not met. The deficiencies in the analysis of low cloud are evident in the recovery of the hit rate up to T+6. However, the false alarm rate is consistently below the UR, and, perhaps

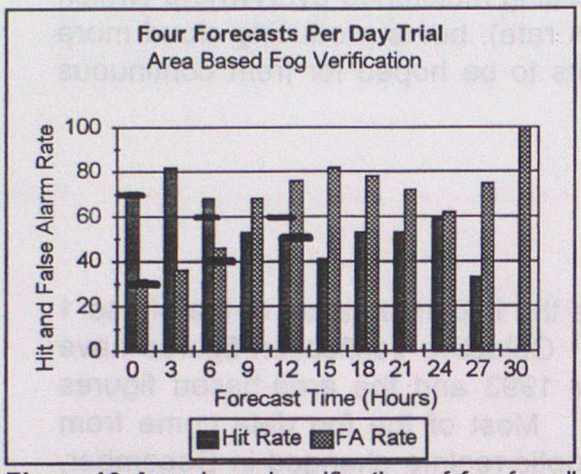

Figure 46 Area based verification of fog for all runs of all cases in continuous assimilation trial.

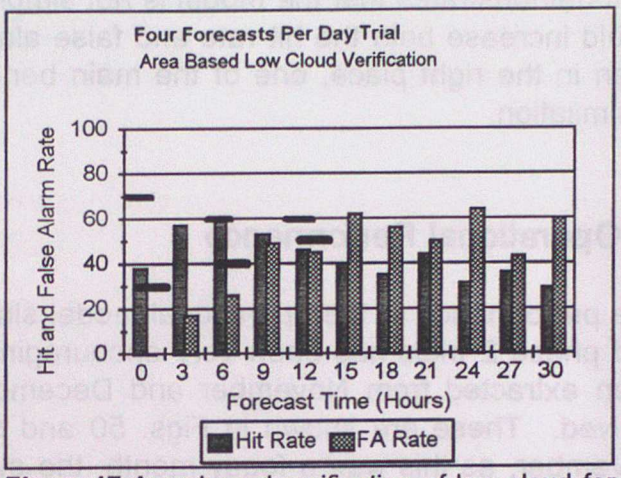

Figure 47 Area based verification of low cloud for all runs of all cases in continuous assimilation trial.

more significantly, below the hit rate (up to T+12), which suggests that a useful signal is present that may achieve the UR with suitable modification of the diagnostic. In fact these figures are let down by the 'stratus' case, on 27 and 28 December 1992 which was chosen as a particularly poor operational case. The 'fog' case chosen which

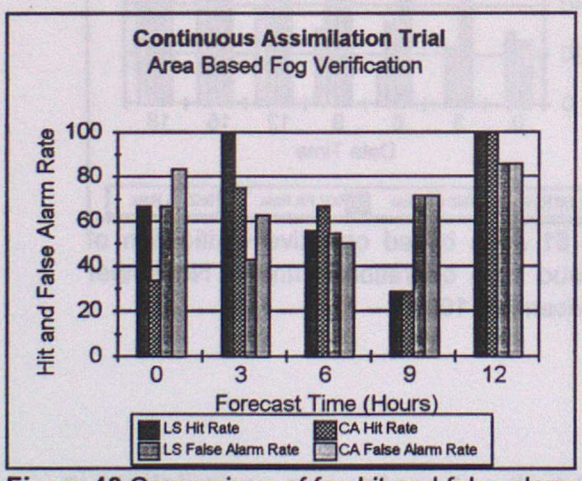

Figure 48 Comparison of fog hit and false alarm rates with and without continuous assimilation.

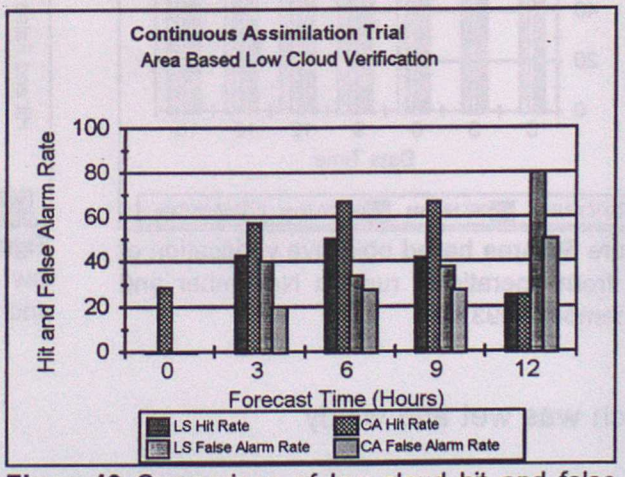

Figure 49 Comparison of low cloud hit and false alarm rates with and without continuous assimilation.

represents straightforward formation of radiation fog overnight, lifting into stratus and dissipation during the morning, performs much better than these figures imply. Indeed, this case, when considered on its own, achieves the UR in all but the hit rate at T+9 (which is only marginally below the requirement) and T+12 (45% rather than 60%).

One run from each case was rerun using the equivalent large scale analysis as the

initial field. The results from the verification are shown in Figs. 48 and 49. It is evident that the impact on fog from continuous assimilation is mixed: indeed it appears that at T+O and T+3 the performance is worse. The 30/04/93 case was tested using the analysis with data time of 18Z on 29/04/93, the first 6 h of which very little fog was present. The hit rate during the first 6 h was therefore dominated by only a few areas and probably does not give a very representative signal. The impact on low cloud is much more clear cut, as the hit rate with continuous assimilation is always greater than without, and the false alarm rate always less. This is particularly encouraging, as it demonstrates that the model is not simply being moistened everywhere (which would increase both the hit rate and false alarm rate), but is producing cloud more often in the right place, one of the main benefits to be hoped for from continuous assimilation.

6. Operational Performance

The performance of the operational model since the implementation of the phase 1 and phase 2 trials has been very encouraging. Objective verification figures have been extracted from November and December 1993 and the area-based figures derived. These are shown in Figs. 50 and 51. Most of the fog data come from November, as this was a foggy month: the synoptic regime changed in December,

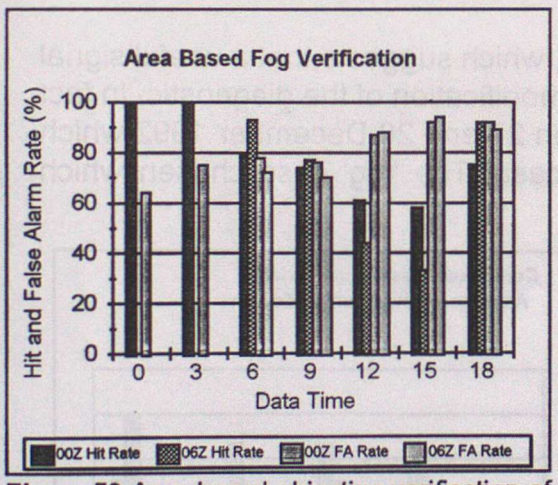

Figure 50 Area based objective verification of fog from operational runs in November and December 1993.

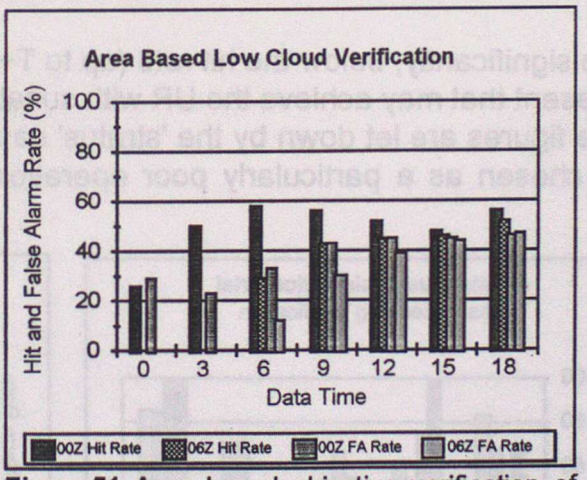

Figure 51 Area based objective verification of low cloud from operational runs in November and December 1993.

which was wet and windy.

The fog performance from the operational model (without continuous assimilation) is similar to, though perhaps somewhat better than, the performance in the trials continuous assimilation. The hit rate is met at T+O and T+6 by, the 00Z forecasts and only falls short by about 5% at T+12. The 06Z forecasts are not quite so good. This may reflect the difference in origin of the initial fields (LAM vs Global) but is also because the 06Z run has the more difficult period (12Z to 18Z) to deal with. The false alarm rate is similarly as much a function of verification time as forecast time. It is high, reflecting the subjective impression that the model is tending to over-forecast,

but it remains less than the hit rate up to T+9 (where they are roughly equal).

The stratus verification behaves quite similarly to the trials: the false alarm rate is low showing a steady growth with forecast time up to T+12, where it levels off at about 45%, while the hit rate starts off poor then remains around 50-55% at all forecast times. The slight peak in hit rate at T+6-9 may reflect the model's known tendency to underdo cloud at analysis time.

The impact of the changes on other parameters is best illustrated by a summary of the CFO subjective assessment. The grades given for precipitation, cloud and 'other' (generally temperature) have been assigned numerical values such that B=O (since B essentially means 'no additional guidance', B+=I, B-=-I etc). The scores are summarized in Figs. 52 to 54. While there is no clear impact on cloud, a step change in score for precipitation in the second half of September (after Phase 1) is very evident. The downward dip in the second half of December may reflect an error in MOPS which was introduced at this time or may simply reflect the synoptic regime which, being dominated by high winds and rain tended to lead to the MM following the LAM quite closely. The 'others' performance is more difficult to assess-. a general upturn in the second half of September may be present but may simply be caused by natural variability. Since the end of December a more specific subjective assessment scheme has been introduced which deals with fog separately.

7. Conclusions

- The modified operational model is providing much improved guidance regarding rainfall, for lower operational cost.

- The performance of the modified mesoscale model is close to the User Requirement for fog and cloud defined in terms of area average fog and low cloud probabilities, although it has not been fully met. The model achieves a good hit rate for fog, and a low false alarm rate for low cloud.

- The performance is very good for the case involving the overnight formation of widespread thick radiation fog, lifting to stratus and dissipating from the edges during the following morning. Performance is poorer for cases involving more patchy fog or stratus formation.

- The area based verification diagnostic, on the whole, gives an impression of performance similar to a subjective assessment and may therefore provide a useful measure of long-term performance.

- The new fog and low cloud diagnostics appear to give a more useful product than visibility charts. In addition, the fog diagnostic provides an indication of the nature of the fog.

- It is anticipated that the implementation of continuous assimilation will generally lead to improved analysis and forecasts, particularly with regard to cloud.

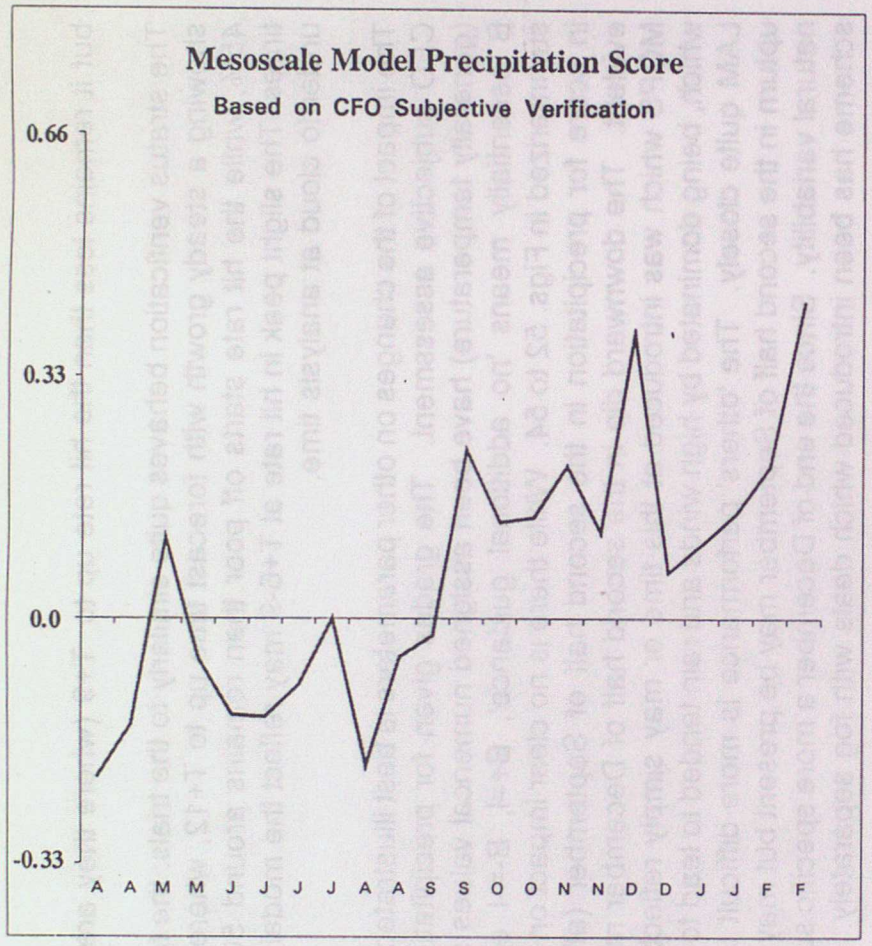

Fig. 52 Precipitation Score based on CFO subjective verification.

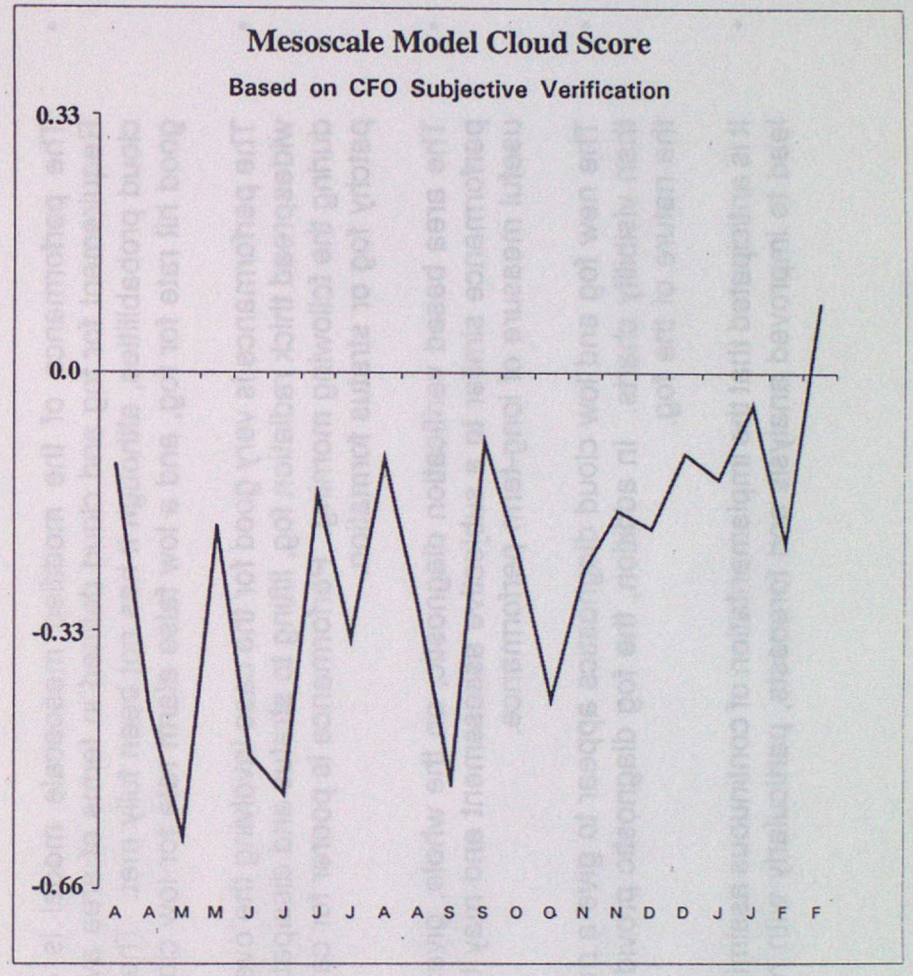

Fig. 53 Cloud Score based on CFO subjective verification.

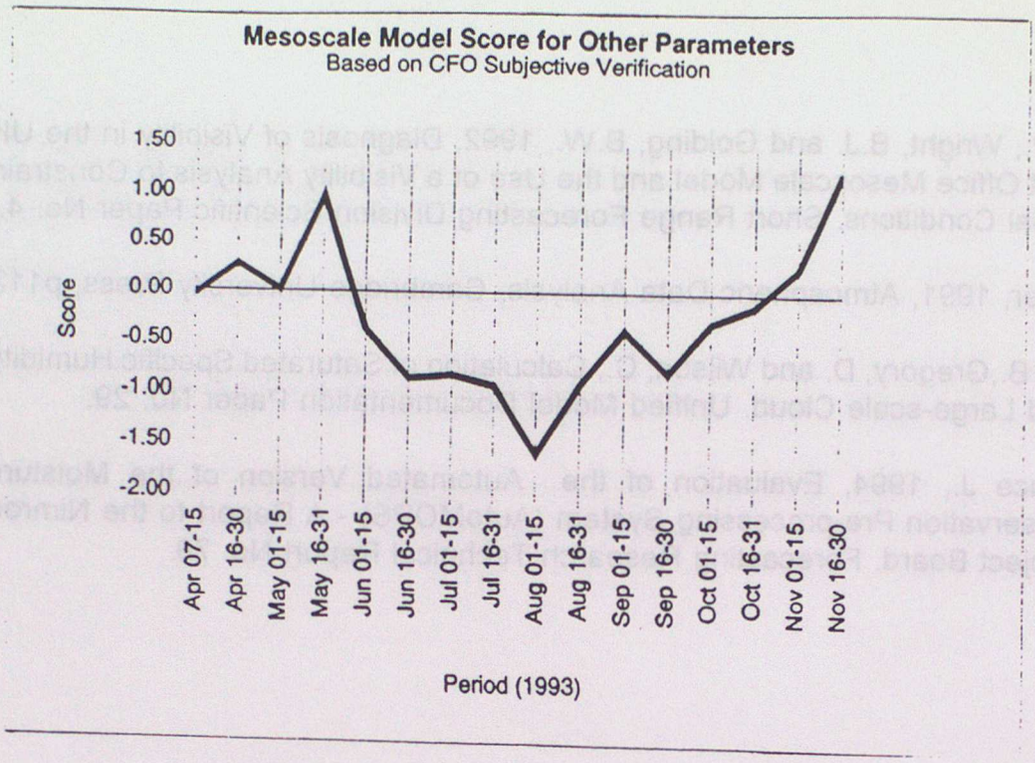

Fig. 54 'Other Parameters' Score based on CFO subjective verification.

References

Ballard, S.P., Wright, B.J. and Golding, B.W., 1992, Diagnosis of Visibility in the UK Met Office Mesoscale Model and the Use of a Visibility Analysis to Constrain Initial Conditions. Short Range Forecasting Division Scientific Paper No. 4.

Daley, Roger, 1991, Atmospheric Data Analysis, Cambridge University Press, p113

Smith, R.N. B.,Gregory, D. and Wilson, C., Calculation of Saturated Specific Humidity and Large-scale Cloud. Unified Model Documentation Paper No. 29.

Wright, Bruce J., 1994, Evaluation of the Automated Version of the Moisture Observation Pre-processing System (AutoMOPS) - A Report to the Nimrod Project Board. Forecasting Research Technical Report No. 79.

Appendix

Level Specifications

The η values for the new levels are shown in the following table, along with the half level entered into the user interface to define them, the level thickness, critical RH and the approximate height in m. The bottom few levels of the original MM are also shown for comparison.

		New Mesoscale Model Levels					Old Mesoscale Model Levels			
Level	Half Level	Eta half	Eta full	Level Thickness	Critical RH	Height (m)	Eta half	Eta full	Level Thickness	Height (m)
	0.5	1.0000					1.000			
1	1.0		0.998800	0.0024	0.9164	10		0.996999	0.0060	25
	1.5	0.9976					0.994			
2	2.0		0.995249	0.0047	0.9082	40		0.989498	0.0090	90
	2.5	0.9929					0.985			
3	3.0		0.988197	0.0094	0.8914	100		0.978495	0.0130	180
	3.5	0.9835					0.972			
4	4.0		0.977696	0.0116	0.8836	190		0.964493	0.0150	300
	4.5	0.9719					0.957			
5	5.0		0.964944	0.0139	0.8754	300		0.948491	0.0170	440
	5.5	0.9580					0.940			
6	6.0		0.948990	0.0180	0.8607	435		0.930488	0.0190	595
	6.5	0.9400								
7	7.0		0.930488	0.0190	0.8571	595				
	7.5	0.9210								
8	8.0		0.910987	0.0200	0.8536	770				
	8.5	0.9010								
9	9.0		0.890485	0.0210	0.8500	955				
	9.5	0.8800								
10	10.0		0.868983	0.0220	0.8500	1155				
	10.5	0.8580								
11	11.0		0.846481	0.0230	0.8500	1365				
	11.5	0.8350								
12	12.0		0.822477	0.0250	0.8500	1600				
	12.5	0.8100								
13	13.0		0.794966	0.0300	0.8500	1870				
	13.5	0.7800								
14	14.0		0.762452	0.0350	0.8500	2200				
	14.5	0.7450								
15	15.0		0.724934	0.0400	0.8500	2600				
	15.5	0.7050								
16	16.0		0.682412	0.0450	0.8500	3080				
	16.5	0.6600								
17	17.0		0.634883	0.0500	0.8500	3640				
	17.5	0.6100								
18	18.0		0.582345	0.0550	0.8500	4300				
	18.5	0.5550								
19	19.0		0.527329	0.0550	0.8500	5050				
	19.5	0.5000								
20	20.0		0.472309	0.0550	0.8500	5870				
	20.5	0.4450								
21	21.0		0.414742	0.0600	0.8500	6800				
	21.5	0.3850								
22	22.0		0.354698	0.0600	0.8500	7900				
	22.5	0.3250								
23	23.0		0.299752	0.0500	0.8500	9040				
	23.5	0.2750								
24	24.0		0.249702	0.0500	0.8500	10260				
	24.5	0.2250								
25	25.0		0.199627	0.0500	0.8500	11750				
	25.5	0.1750								
26	26.0		0.149502	0.0500	0.8500	13700				
	26.5	0.1250								
27	27.0		0.099247	0.0500	0.8500					
	27.5	0.0750								
28	28.0		0.056855	0.0350	0.8500					
	28.5	0.0400								
29	29.0		0.029595	0.0200						
	29.5	0.0200								
30	30.0		0.014797	0.0100						
	30.5	0.0100								
31	31.0		0.004606	0.0095						
	31.5	0.0005								